Identification of regulators of heat shock-inducible gene in *Arabidopsis*

by

Qingxia Ruan, M. S.

A Thesis
In

CHEMISTY AND BIOCHEMISTY

Submitted to the Graduate Faculty
of Texas Tech University in
Partial Fulfillment of
the Requirements for
the Degree of

MASTER OF SCIENCES

Approved

Shi, Huazhong
Chair of Committee

Xie, Zhixin

Paul, Pare

Dominic Cassadonte
Interim Dean of the Graduate School

December, 2012

ACKNOWLEDGEMENTS

The research work of identifying the polyamine uptake transporter gene is conducted in Dr. Shi's lab. I want to thank Dr. Shi for providing me the opportunity to do the research in his lab using *Arabidopsis* as the model and all the possible support and facilities such as the luciferase imaging system for screening the mutants. Also, I want to thank him for the suggestions and help. Besides, I am thankful for the 9 months of RA support. In addition, I would like to thank the senior graduate students in the lab for their help and opinions. At last, I also want to thank Dr. Xie for expanding my knowledge in the small RNA course and his patience for my discussions with him about the research and the study in the class. And I want to thank Dr. Pare for his help and advice on my study and research.

TABLE OF CONTENTS

ACKNOWLEDGEMENTS ..... **ii**

ABSTRACT ..... **vi**

LIST OF TABLES ..... **vii**

LIST OF FIGURES ..... **viii**

LIST OFABBRIEVATIONS ..... **ix**

I. INTRODUCTION **1**

1. 1 Heat stress and heat shock proteins 1

1. 2 Heat inducible gene *At5g59720* and its regulation by Hsfs 4

1. 3 *At5g59720* gene expression is highly induced by heat stress 5

1. 4 The change of chromatin structure in *At5g59720* gene after heat induction 6

1. 5 Forward genetics screening 6

II. MATERIALS AND METHODS **15**

2. 1 Construction of *At5g59720P: LUC* fusion gene and *Agrobacterium* mediated plant transformation 15

2. 2 Luciferase imaging of transgenic Arabidopsis T2 population 16

2. 3 Screen single locus T-DNA transformant in *Arabidopsis* T2 population 16

2. 4 Screen homozygous transgenic lines with single *T-DNA* insertion in *Arabidopsis* T3 population 16

2. 5 EMS mutagenesis of the homozygous *At5g59720P: LUC* transgenic line 17

2. 6 Screening mutants showing altered luciferase expression 17

2. 7 Confirmation of the screened *CH*, *HL* and *LL* class mutants 17

2. 8 Screening methyl viologen resistant mutants 18

2. 9 Screening methyl viologen resistant *LL729*×Ler F2 mapping population 18

2. 10 Positional cloning to identify the mutation in *LL729* 18
2. 10. 1 Rough mapping 18
2. 10. 2 Fine mapping 19

2. 11 DNA sequencing of the candidate genes in *LL729* mutant 19

2. 12 Complementation of luciferase imaging phenotype of *LL729* 19

2. 13 Heat stress treatment 20

2. 14 Other abiotic stress treatment 20
2. 14. 1 Cold stress treatment 20
2. 14. 2 Salt stress treatment 20
2. 14. 3 Osmotic stress treatment 20

III. RESULTS 24
3. 1 *Arabidopsis* transgeic line T_3-5-4 is a homozygous line with a single locus of T-DNA insertion 24

3. 2 Screened *CH*, *HL* and *LL* class mutants 24

3. 3 *LL729* is a lower luciferase expression mutant 24

3. 4 *LL729* mutant is resistant to methyl viologen 25

3. 5 *LL729* has no obvious thermotolerant or thermosensitive phenotype 25

3. 6 Effects of other abiotic stresses on the induction of *At5g59720* promoter-luciferase fusion gene in the mutant *LL729* and the control line 25

3. 6. 1 Cold stress treatmenton the induction of *At5g59720* promoter-luciferase transgene ... 25
3. 6. 2 Salt stress treatments on the induction of *At5g59720* promoter-luciferase transgene . 26
3. 6. 3 Osmotic stress treatments on the induction of *At5g59720* promoter-luciferase transgene 26

3. 7 Mutation in *LL729* is localized in the gene *At5g05630* 26
3. 7. 1 Screen the methyl viologen resistant *LL729* × Ler F2 population 26
3. 7. 2 Rough mapping 26
3. 7. 3 Fine mapping 27
3. 7. 4 DNA sequencing of candidate genes 27

3. 8 PUT3 transmembrane domain prediction 27

3. 9 Exogenous polyamines increase luciferase expression in the mutant *LL729* at normal growth conditions 28

3. 10 Exogenous polyamines do not increase luciferase expression in the mutant *LL729* after heat induction 29

3. 11 Complementation of *LL729* luciferase imaging phenotype..... 29

IV. CONCLUSIONS AND DISCUSSIONS 45

4. 1 Mutation of Ser_{252} to Asn_{252} in PUT3 affects its transporting activity in *LL729* and renders it resistant to methyl viologen..... 45

4. 2 Mutation of Ser_{252} to Asn_{252} in PUT3 affects its transporting activity of polyamines in *LL729*..... 46

4. 3 Decreased intracellular polyamines reduce basal and induced expressions of heat-inducible genes in *LL729* and the possible mechanisms 47

REFERENCES..... 56

APPENDICES..... 61

A. THE INTERACTING COMPONENTS LISTED IN THE NETWORK OF FIGURE 1. 5..... 61

ABSTRACT

By using forward genetic screening, we identified an *Arabidopsis* mutant *LL729* showing reduced expression of the luciferase reporter gene driven by the heat stress inducible promoter of AtHsp18.2 gene. Extensive phenotyping of the *LL729* mutant revealed that *LL729* is resistant to the toxic non-selected herbicide methyl viologen. Through positional cloning, we found that the mutation responsible for the *LL729*'s luciferase imaging and methyl viologen resistant phenotypes is localized in *At5g05630* encoding a polyamine uptake transporter named PUT3. We deduce that the mutation resulting in a change of $serine_{252}$ to $asparagine_{252}$ in the PUT3 reduced the transport of methyl viologen as well as polyamines into *Arabidopsis.*

LIST OF TABLES

2. 1 Markers used for fine mapping to narrow down the mutation locus in mutant *LL729*.....22

4. 1 Sequence alignment of polyamine uptake transporter homologs in *Arabidopsis*.....51

4. 2 Molecular formula of methyl viologen and its analog polyamines 52

LIST OF FIGURES

1. 1 AtHsp18.2 amino acid sequence and the double disk model of dodecamer of AtHsp 18.2 based on the crystal structure template of Hsp16.9.....30

1. 2 Phylogenetic analysis of sHsps 30

1. 3 Phylogenetic analysis of Hsfs 30

1. 4 Phylogenetic analysis of 21 members of *Arabidopsis* Hsfs.....12

1. 5 Interacting networks of AtHsp18.2, HSF1 (AtHsfA1a), AtHsfA1b, and AtHsfA2 in *Arabidopsis* 13

1. 6 Illustration of AtHsp18.2 heat shock elements on its promoter.....14

2. 1 Construction of *At5g59720* promoter-luciferase fusion using pCAMBIA1381-LUC vector.....30

3. 1 Confirmation of single locus and homozygous T-DNA transgenic line T_3-5-4 by luciferase imaging.....30

3. 2 Confirmation of *LL729* mutant phenotype in the second generation 30

3. 3 Luciferase imaging phenotype of *LL729* 30

3. 4 Methyl viologen resistant phenotype of *LL729* 30

3. 5 Phenotype of *LL729* after heat stress treatment 30

3. 6 Abiotic stress treatment of the background line T_3-5-4 and *LL729*.....30

3. 7 Chromosomal walking to identify the mutation locus in *LL729* 30

3. 8 Amino acid sequence of PUT3 and the DNA sequencing result of gene *At5g05630* 30

3. 9 TMHMM prediction of PUT3 transmembrane helical domains and representation by TMRPres2D 40

3. 10 Predicted tertiary structure of PUT3 by FFAS03 based on template 3ncy.....41

3. 11 Polyamines affect the luciferase activities in *LL729* and the background line T_3-5-4. 42

3. 12 Complementation of luciferase imaging phenotype 45

4. 1 Phylogenetic tree prediction of polyamine uptake transporter homologs in *Arabidopsis* 53

4. 2 Illustration of amino acid residue post-translational modification on histone 3 and histone 4 54

4. 3 Model of histone acetylation affecting gene transcription.....55

LIST OF ABBRIEVATIONS

AHA	aromatic/hydrophobic/acidic motif
ASN	asparagine
APC	amino acid-polyamine-organocation
BiFC	bimolecular fluorescence complementation
CH	constitutively higher luciferase expression
CCD	charge coupled device
cDNA	complementary deoxynucleotide acid
DNA	deoxynucleotide acid
CaM	calmodulin
CBK	calmodulin binding kinase
CDC2	cyclin-dependent protein kinase
ChIP	chromatin immunoprecipitation
EMS	ethyl methanesulfonate
EMSA	electrophoretic mobility shift assay
Fd	ferrodoxin
FFAS	fold and function assignment
FRET	fluorescent resonance energy transfer
HL	higher luciferase expression
Hsf	heat shock transcription factor
HSP18.1-CI	heat shock protein 18.1 class I
HSP83	heat shock protein 90.1
LB	Luria-Bertani
LUC	firefly luciferase gene
LL	lower luciferase expression
M_1	mutant generation one
M_2	mutant generation two
MS	murashige-skoog basal salt
PUT3	polyamine uptake transporter 3

RNA	ribonucleotide acid
ROF1	rotamase FK506 binding protein 1
ROS	reactive oxygen species
Ser	serine
SUMO1	small ubiquitin-like modifier 1
SWI/SNF	switch/sucrose non fermentable
TBP1	TATA binding protein 1
TBP2	TATA binding protein 2
TSS	transcription start site
T_2	transgenic generation two
T_3	transgenic generation three
T-DNA	transferred DNA
TFIID	RNA polymerase II transcription factor D
TM	transmembrane domain
TMHMM	transmembrane protein topology in Hidden Markov model
TMRPres2D	TransMembrane protein Re-Presentation in 2Dimensions
5'-UTR	5' un-translated region

CHAPTER I
INTRODUCTION

Arabidopsis is a commonly used model plant nowadays in research due to its small size of genome (Leutwiler et al., 1984), lower repetitive DNA sequences, and mostly single copy genes (Pruitt et al., 1986). It is a model for studying how plants respond to the external environmental stresses such as heat stress, cold stress and other abiotic stresses (Zhu 2002; Hirayama et al., 2010). Intensive studies in this field have significantly enhanced our understanding on how plants cope with different environmental stresses by employing multiple regulatory pathways targeting distinct steps in the gene expression process ranging from transcriptional regulation, post-transcriptional processing, mRNA degradation, translation, post-translational processing, protein targeting and transport, to protein degradation.

1. 1 Heat stress and heat shock proteins

Heat stress is a kind of typical environmental stress which exists widely in the environment and poses a lot of threats to plants and animals. Heat stress can cause a series of disorders and damages for the cellular system, for instance, it can disrupt the membrane system such as the plasma membrane and mitochondrial membrane and so on, leading to the release of cytochrome c, production of reactive oxygen species (ROS) that cause oxidative stress to the cellular organelles, proteins and other cellular components (Larkindale et al., 2002). Heat stress can trigger the organism to produce a series of products, such as heat shock family proteins or anti-oxidant enzymes and a series of effectors such as mitogen activated protein kinases and phosphatases involved in the signal transduction pathways to help protecting them from the stress (Larkindale et al. 2005b; Kotak et al., 2007; Mishkind et al., 2009).

Heat shock protein families are the major products that are produced by cells when they are under heat stress. It is known that Hsp superfamily include five families.

Hsp101 family, Hsp90 family, Hsp70 family, Hsp60 family and small heat shock proteins (sHsps) family based on their molecular weight (Georgopoulos et al., 1993; Whitley et al. 1999; Sun et al., 2005). *Arabidopsis* also possesses this superfamily including the sHSPs family (Swindell et al., 2007). Each heat shock protein family contains more than one member in *Arabidopsis*. For instance, Hsp70 family contain at least 13 members ranging from Hsp70-1 to Hsp70-17 (Swindell et al., 2007), sHsps contain at least 19 annotated members, including Hsp18.1-CI, Hsp17.8-CI, Hsp17.4-CII and so on (Siddique et al., 2008).

The small Hsps usually form oligomer and perform their functions in the cytosol (Sun et al., 2005). Figure 1. 1 shows the predicted structure of AtHsp18.2 dodecamer based on the template structure and the amino acid sequence of AtHsp18.2. The phylogenetic tree (Figure 1.2) shows the evolutionary relationships of small Hsps such as Hsp18.1-CI (Hsp 18.2), Hsp17.8-CI, Hsp17.4-CII.

Under heat stress, heat shock proteins play important roles inside the cells to maintain the normal functions of cells such as helping refolding the denatured protein to their native structures and preventing the aggregation of protein under the heat stress condition thus maintaining the protein in an active conformation and form (Georgopoulos et al., 1993; Whitley et al., 1999). In addition, Hsps are also involved in the developmental regulation and protein transportation and targeting inside the cell. Many of the heat shock genes' promoters contain the heat shock transcription factor (Hsf) binding site called heat shock element (HSE) located in front of the transcription start site (TSS) (Nover et al., 2001). Therefore, upon heat stress, the promoters of heat shock genes can be bound by heat shock transcription factors and the transcription becomes activated.

Through structural analysis and phylogenetic comparison, 3 classes and 14 groups of heat shock transcription factors were identified in *Arabidopsis*. *Arabidopsis* Hsfs include 15 members of class-A subfamily AtHsfs, 5 members of class-B subfamily AtHsfs and 1 class-C subfamily AtHsfC1 (Nover et al., 2001). Figures1.3 shows the phylogenetic tree displaying the evolutionary relationships of Hsfs in plants and Figure

1.4 specifically shows the phylogenetic analysis of 21 Hsfs members in *Arabidopsis*. HsfA class can directly bind to heat shock elements (HSEs) located on the promoters of heat shock genes and activate the transcription of heat shock genes through their aromatic/hydrophobic/acidic domain (AHA) interacting with RNA polymerase II. AtHsfB and AtHsfC classes do not directly activate the transcription of heat shock genes due to lack of AHA activation domain, but they can bind with AtHsfA class to affect the AtHsfA class's activation of heat shock gene transcription (Li et al., 2010). In addition to heat shock transcription factors, studies using yeast two hybridization, FRET (fluorescence resonance energy transfer) and BiFC (Bimolecular fluorescence complementation) revealed that some other mediators such as AtCaM3 (calmodulin), calmodulin binding kinase (like AtCBK3) and serine/theronine phosphatase (PP7) can interact with AtHsfs like AtHsfA1a and AtHsfA2 to affect their post-translational modification such as phosphorylation and hence oligomerization of AtHsfs upstream of AtHsfs binding with HSEs (Liu et al., 2005; Liu et al., 2008). However, the components that are involved in the heat signal transduction pathway are not completely discovered and illustrated, i.e, the transmembrane proteins involved in protein or substance transportation, members involved in protein targeting, enzymes involved in the synthesizing or degrading the substances important for the heat signal transduction pathways and so on.

Therefore, our research focuses on using *Arabidopsis* as a model system, by using a heat inducible promoter from the heat shock inducible gene *At5g59720* fused with the luciferase (LUC) reporter gene in combination with a high sensitive LUC imaging system to study how heat shock inducible genes are regulated. This study could identify important regulators in the heat signal transduction pathways and elucidate the molecular mechanisms of plant heat stress response and adaptation.

1. 2 Heat inducible gene *At5g59720* and its regulation by Hsfs

Arabidopsis heat shock gene *At5g59720* encodes the small heat shock protein AtHsp18.2belonging to a small heat shock protein class. The interaction network of AtHsp18.2 in *Arabidopsis* is shown in Figure 1.5. The expression of heat shock gene *At5g59720* can be up-regulated by heat shock transcription factors such AtHsfA1a, AtHsfA1b and AtHsfA2 and so on. Through S1 enzyme digestion and ChIP assay, it was found that heat shock gene *At5g59720* contains 6 repeat of heat shock elements (HSEs), three HSEs are located at the proximal site of *At5g59720* transcription start site (TSS), the other three HSEs are located at the distal site of TSS (Figure 1. 6) (Kodama et al., 2007). Each HSE of *At5g59720* contains a conserved sequence of5'-GAAnnCTTnnAAG-3' or 5'nTTCnnGAAnnTTCn3 (Li et al., 2010) and this sequence can be recognized and bound by an active homotrimer of AtHsfA1a or AtHsfA2, or an active heterotrimer of AtHsfA1a/1b to enhance the transcription of heat shock gene *At5g59720* under heat induction. In order to determine which HSEs is bound by AtHsfA1a, through enzyme digestion, ChIP assay followed by quantitative PCR, it was found that AtHsfA1a homotrimer preferably bind to the proximal sites of three HSEs (Kodama et al., 2007).

AtHsfA1a and AtHsfA1b are two lower constitutively expressed heat shock transcription factors which exist in the cytosol and act as the early responding AtHsfs to up-regulate the transcription of heat shock genes *At5g59720* under heat stress. Without heat stress, AtHsfA1a and AtHsfA1b inside the cytosol are inactive due to their binding with Hsp70-1 and Hsp-4 which blocks the functions of each other (Kim et al., 2002). When cells are under heat stress, a lot of proteins inside the cells start to become denatured and lose their natural conformation, the cells produce stress signals to signify heat shock protein Hsp70 to dissociate with its binding partners such as AtHsfA1a or AtHsfA1b to refold the denatured protein. The released individual monomer of AtHsfA1a or AtHsfA1b can be further phosphorylated by the relative kinase at Ser residue and then trimerize to form an active homotrimer and translocated to the nucleus to bind to heat shock element on the promoter of heat shock gene *At5g59720* and enhance the transcription during an early stage of heat stress.

Besides the early enhancement by AtHsf1a or AtHsf1b, the transcription of *At5g59720* is also largely enhanced by a later responding heat shock transcription factor-AtHsfA2 under heat stress (Li et al., 2010). The expression of AtHsfA2 is not constitutive but inducible by heat stress. There is a signal cascade that exists upstream of AtHsfA2 transcription under heat stress and it is known that AtHsfA1 can induce the transcription of AtHsfA2 (Li et al., 2010). AtHsfA2 plays an important role for the extension of *Arabidopsis* resistant to heat stress (Li et al., 2010). It is also known that AtHsfA2 and AtHsfA1a can form a hetero-oligomer and can still activate the transcription of heat shock gene *At5g59720* (Li et al., 2010). The interaction network of AtHsf A1a, AtHsfA1b and AtHsfA2 as well as AtHsp18.2 in *Arabidopsis* can be viewed in Figure 1. 5.

1. 3 *At5g59720* gene expression is highly induced by heat stress

Based on the luciferase imaging characterization, we found that the luciferase expression driven by the heat shock gene *At5g59720* promoter can be induced more than 10 folds after 40°C treatment for 1h than the control without heat stress. The induction of *At5g59720* gene expression by heat stress is also evidenced by the microarray analysis (Swindell et al., 2007). In addition to heat stress, *At5g59720* can be induced to different extents by other abiotic stresses like cold stress, UV stress, osmotic stress and so on. Therefore, it is a good system for us to study the regulation of heat shock protein under heat stress and can also be used to study the network of how other stresses affect the expression of *At5g59720*.

1. 4 The change of chromatin structure in *At5g59720* gene after heat induction

The chromatin structure of *At5g59720* gene was shown to be changed after heat stress treatment. In a ChIP assay, 30°C treatment of cells for 0.5h resulted in2-fold lower H3 occupancy at the *At5g59720*'s promoter and coding sequence region compared to the H3 occupancy without heat treatment, also the H3K9 and H3K14 acetylation status increased by 1.6 fold after heat treatment (Kodama et al., 2007) compared to that before heat treatment. How is the chromatin structure remodeled during gene transcription, such as the relationships of Hsfs binding with HSE, histone acetylation and histone occupancy? Strenkert et al (2011) studied Hsp25 gene and found that the binding of Hsf1 to the HSE region (no histone occupied) occurs first and followed by the promotion of H3 acetylation and losing contact with the promoter and the reduced H3 occupancy due to the removal of histone by the relative remodeling complex.

1. 5 Forward genetics screening

In our system, we used the forward genetic screening method attempting to identify regulators that are involved in the heat signal transduction pathways. The basic procedure is as follows: i) create the transgenic *Arabidopsis* by using our interest gene's promoter fused with a reporter gene that can be used to track gene expression**;** ii) EMS mutagenesis to create mutations in the genome causing disruption of gene functions. The EMS mutation can usually result in a single nucleotide change from guanine to adenine and this conversion is retained during the following DNA replication and meiosis. If the single nucleotide mutation is a mis-sense mutation or non-sense mutation, then it can change the normal functions of the gene's products; iii) screen the appropriate mutants based on the phenotype we are interested to study and confirm the phenotypes of the mutants in the second generation; iv) positional cloning to identify the mutated gene; and iv) complementation of the mutant phenotype.

At Hsp18.2

MSLIPSIFGGRRSNVFDPFSQDLWDPFEGFFTPSSALANASTARDVAAFTNARVD
WKETPEAHVFKADLPGLKKEEVKVEVEDKNVLQISGERSKENEEKNDKWHRVE
RASGKFMRRFRLPENAKMEEVKATMENGVLTVVVPKAPEKKPQVKSIDISGAN

(A)

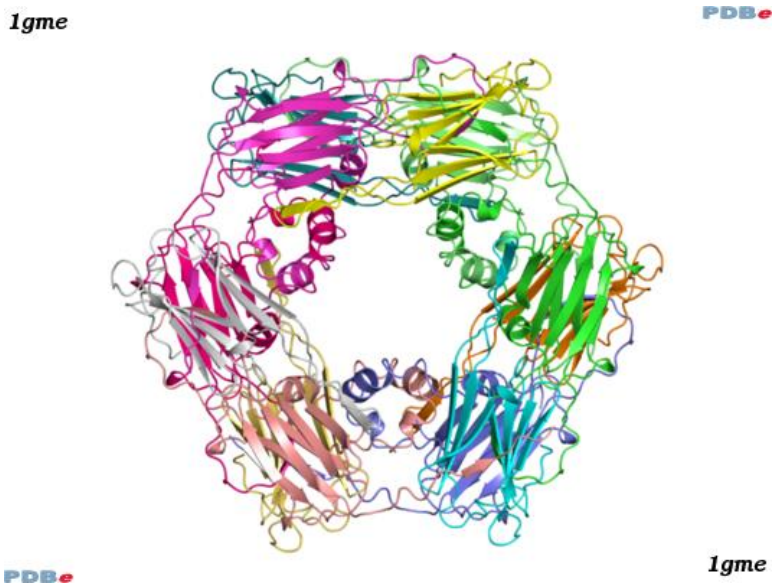

(B)

Figure 1. 1 AtHsp18.2 amino acid sequence and the double disk model of dodecamer AtHsp18.2 based on the crystal structure template of Hsp16.9. **(A)** AtHsp18.2 amino acid sequence. **(B)** The double disk model of dodecamer AtHsp18.2 based on the crystal structure template of Hsp16.9 with the protein data bank entry of 1gme.pdb. The structure model is adapted from http://swissmodel.expasy.org/repository/?pid=smr03&mid=mee6ac4c819de67b6eebaaa558812884d_s51_e159_t1gme.

Figure 1. 2 Phylogenetic analysis of small HSPs. The phylogenetic analysis is adapted from PhylomeDB database with the link http://phylomedb.org/?seqid=P19037.

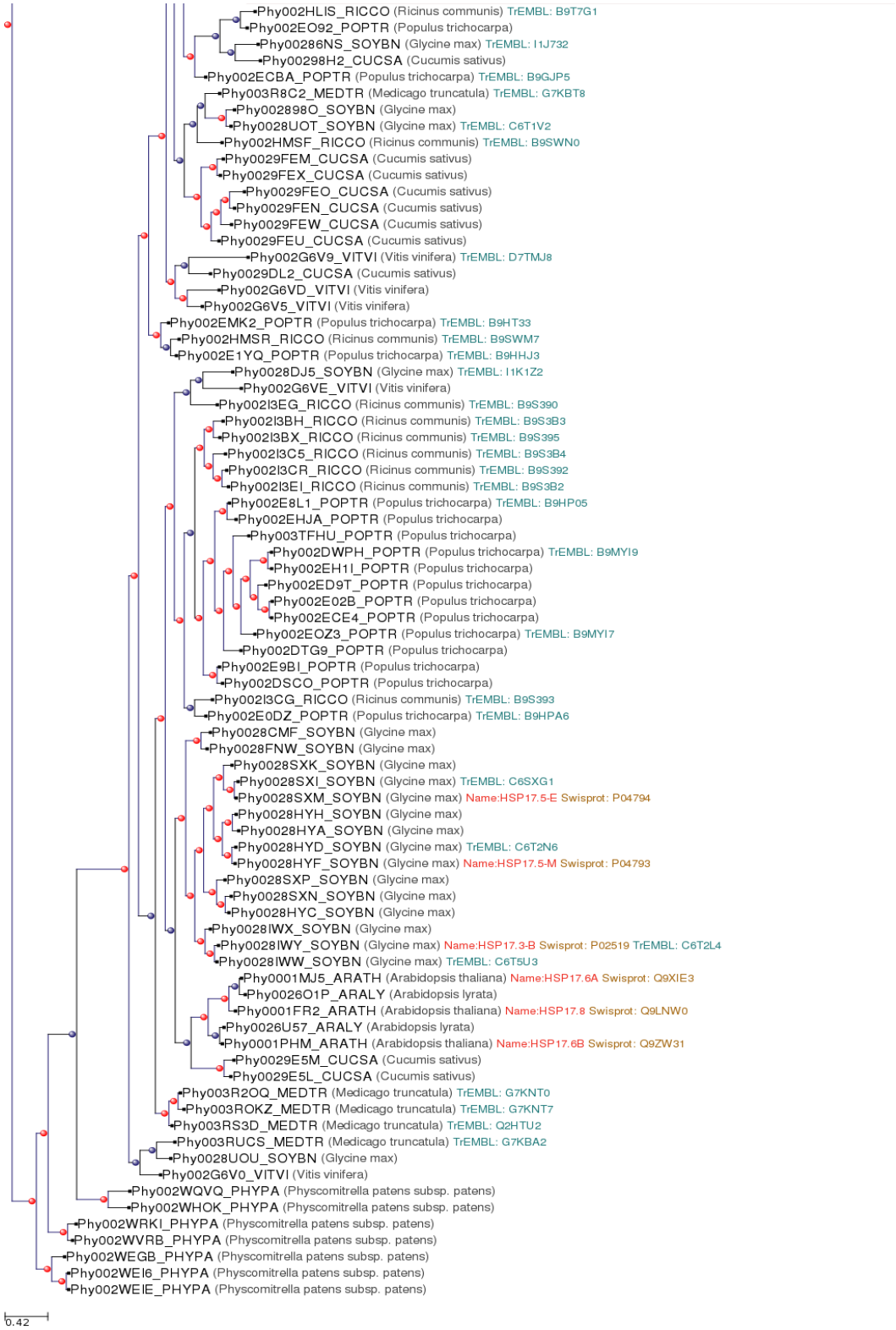

Figure 1. 2 Continued.

Figure 1. 3 Phylogenetic analysis of Hsfs. The analysis is adapted from PhylomeDB database with the link of http://phylomedb.org/?seqid=P41151.

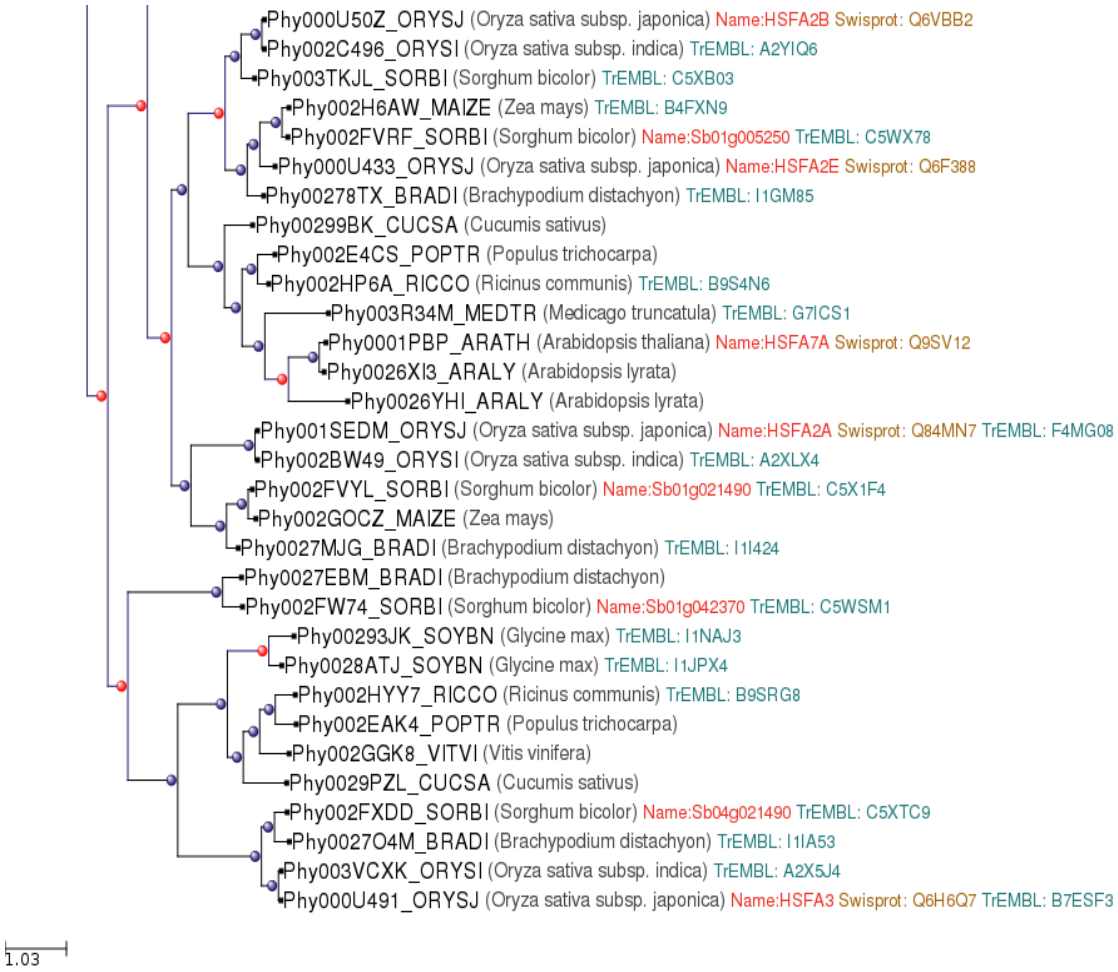

Figure 1. 3 Continued.

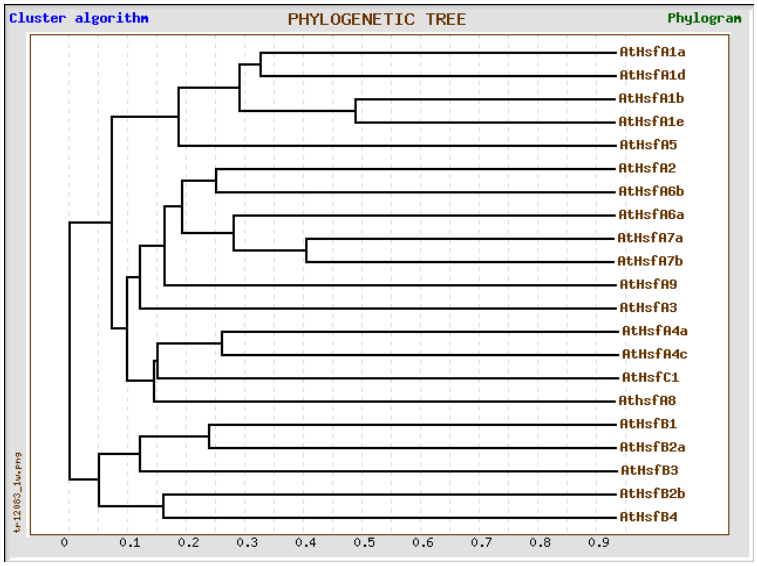

(A)

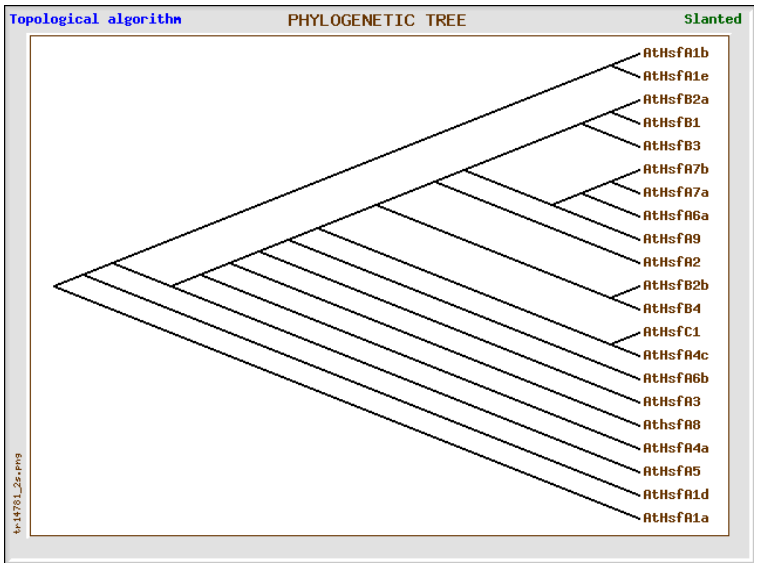

(B)

Figure 1. 4 Phylogenetic analysis of 21 members of *Arabidopsis* Hsfs. Using cluster algorithm **(A)** and topological algorithm **(B)**. The analysis is done by genebee software with the link http://www.genebee.msu.su/services/phtree_reduced.html.

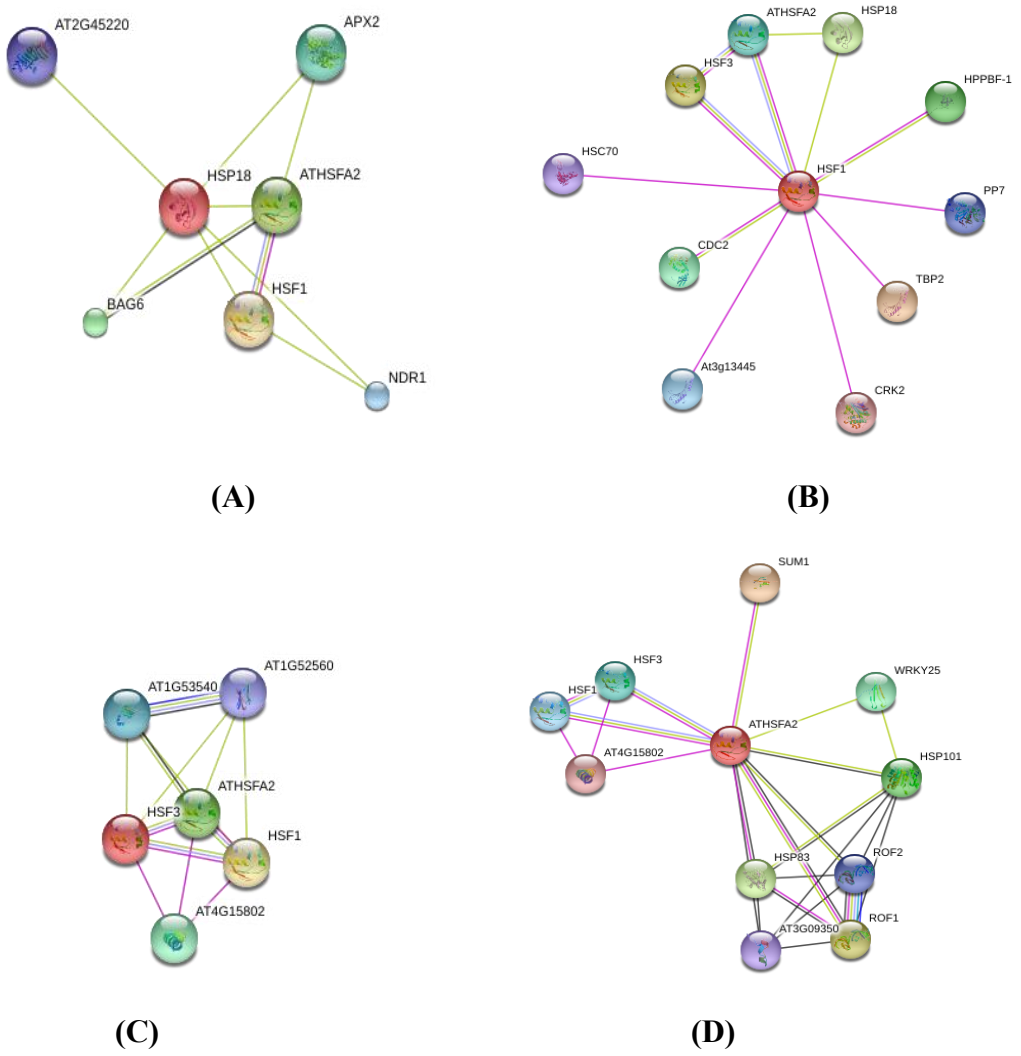

Figure 1. 5 Interacting networks of AtHsp18.2 **(A)**, HSF1 (AtHsfA1a) **(B)**, AtHsfA1b **(C)**, AtHsfA2 **(D)** in *Arabidopsis.* (pink) indicates the actual protein-protein interactions verified by experiments, (blue) means concurrence of two components.

The figures are adapted from the string protein-protein interaction databases with the following links, respectively:

(A) http://string-db.org/newstring_cgi/show_network_section.pl?identifier=P19037;

(B) http://string-db.org/newstring_cgi/show_network_section.pl?identifier=P41151;

(C) http://string-db.org/newstring_cgi/show_network_section.pl?identifier=O81821;

(D) http://string-db.org/newstring_cgi/show_network_section.pl?identifier=O80982.

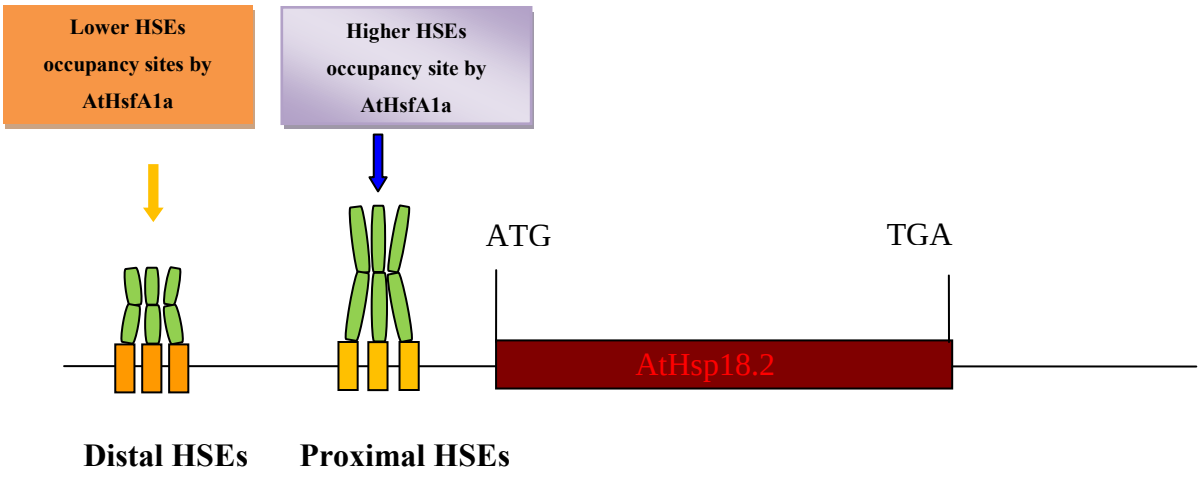

Figure 1. 6 Illustration of AtHsp18.2 HSEs elements on its promoter.

CHAPTER II

MATERIALS AND METHODS

2. 1 Construction of *At5g59720P: LUC* fusion gene and *Agrobacterium* mediated plant transformation

A transcriptional fusion of *At5g59720* promoter with the *LUC* reporter gene was constructed based on a luciferase reporter carrier plasmid-pCAMBIA1318Z-LUC. In brief, *Arabidopsis At5g59720* gene's promoter and 5' un-translated region (5'-UTR) was amplified from *Arabidopsis* genomic DNA by using forward primer: 5'cgggatccGCTTTGACGACAAGTAGGTTTGTTC-3'and reverse primer: 5' aaaactgcagTGTTCGTTGCTTTTCGGGAG-3'. Then the PCR amplified products about 900 bp were ligated to the pCAMBIA1318Z-LUC vector at two restriction sites in front of the luciferase coding sequence to create *At5g59720P: LUC* fusion gene (see Figure 2. 1).

The constructed plasmid of 5*g59720P: LUC*T-DNA was confirmed by DNA sequencing and then introduced to *Agrobacterium tumefaciens* by electroporation. The transformants of *Agrobacterium* was selected on LB (l0g tryptone, 5g yeast extract, 10g NaCl, pH=7.0) medium with kanamycin antibiotics at 30°C for 12~16 hours. Then *Agrobacterium* transformants were transferred to liquid YEP medium (10g yeast extract, 10g Bacto peptone, 5g NaCl, pH=7) for further growth at 30°C for 12 ~16 hours and used for plant transformation. The un-opened flower buds of *Arabidopsis* growing about 1 month-old were incubated with the *Agrobacterium* suspension solution in 500mL (1/2 × Murashige-Skoog, 5% sucrose, 200µl silwat-77, pH=5.7) for 1 min and then covered with a transparent plastic dome to maintain the humidity for overnight. The seeds collected from the T-DNA transformed *Arabidopsis* were used for screening the T1 transgenic plants. The seeds from individual T1 transgenic lines (called T2 generation) were used for selection of transgenic lines with single T-DNA insertion.

2. 2 Luciferase imaging of transgenic *Arabidopsis* T2 population

Luciferase imaging of transgenic *Arabidopsis* was carried out as follows: transgenic *Arabidopsis* seeds of T2 generation were sterilized and planted on half strength Murashige-Skoog medium (0.7% agar, 1.5% sucrose, 1/2 × Murashige-skoog salt, pH=5.7) to grow at 22°C under a 16-h light/8-h dark cycle for 7 days. Then the seven-day-old seedlings were sprayed with 1mM D-luciferin and incubated in dark for 5 minutes and transferred to the dark chamber for incubation of another 2 minutes to quench the autofluorescence emitted by chlorophyll. Then the intensity of bioluminescent emitted from oxylucifin catalyzed by luciferase using D-luciferin as the substrate was detected by a cooled charge-coupled device (CCD) camera located at the top of the chamber, the capture time is usually 5min. The relative luciferase activity was judged by the maximum bioluminescent counts detected by CCD camera for each individual seedling.

2. 3 Screen single locus *T-DNA* transformant in *Arabidopsis* T2 population

Arabidopsis seeds collected from T1 transformants are called T2 generation. T2 seeds collected from each single T1 plant were sterilized and planted on 1/2 MS medium and grow at 22°C with a16h-light/8h- dark cycle for seven days on the growth shelf. The single locus T-DNA insertion in *Arabidopsis* genome was judged by the bioluminescent segregation ratio of 3:1 (bioluminescence: no bioluminescence) generated from the T2 populations.

2. 4 Screen homozygous transgenic lines with single *T-DNA* insertion in *Arabidopsis* T3 population

About eight different seedlings expressing luciferase were randomly selected from the three fourth population of each transgenic line and transferred to pot to grow for transgenic *Arabidopsi*s T3 generation which was further used for isolation of homozygous transgenic lines. T3 seeds collected from each individual T2 plant were sterilized and planted on the same 1/2 MS medium, respectively, to grow seven days and were subjected to luciferase imaging as the same method described above. The T3

transgenic lines showing no segregation for luciferase gene (all show bioluminescence) were selected as homozygous transgenic lines for further study.

2. 5 EMS mutagenesis of the homozygous *At5g59720P: LUC* transgenic line

The seeds collected from the homozygous transgenic line (named T_3-5-4) were treated with EMS to generate genome-wide mutations. 0.5g of the transgenic *Arabidopsis* seeds were treated with 0.3% EMS solution on a shaker for 16 hours. The EMS treated seeds (M1) are then divided into 15 pools and grown in the growth room at 22°C with a 16 h-light/8h-night cycle to obtain M2.

2. 6 Screening mutants showing altered luciferase expression

M_2 seeds of T_3-5-4 collected from those 15 different pools are sterilized and planted on 1/2 MS medium for 7 days and are further subjected for screening of mutants showing constitutively higher luciferase expression at normal growth conditions or with lower or higher luciferase expression after heat treatment based on their luciferase activities by luciferase imaging. The T_3-5-4 line was used as the control when screening for mutants showing different luciferase activities. Mutants showing constitutively higher luciferase expression without heat induction were picked out and named with an ordered number preceded by a prefix *CH* (constitutively higher luciferase expression). Mutants showing higher or lower luciferase expression based on the intensity of bioluminescent emission after 40°C induction for 1h were also selected and labeled with a consecutive number preceded by a prefix *HL* (higher luciferase expression) or *LL* (lower luciferase expression). These putative mutants were then transferred to soil and continue to grow to obtain seeds in order to confirm their luciferase imaging phenotypes in the next generation.

2. 7 Confirmation of the screened *CH*, *HL* and *LL* class mutants

Confirmation of *CH* class mutants in the second generation was carried out by determining luciferase expression in the mutants at normal growth conditions using

luciferase imaging. Confirmation of screened *HL* and *LL* class mutants was carried out by luciferase imaging of the mutants after 40°C heat induction for 30minutes or 1h.

2. 8 Screening methyl viologen resistant mutants

For screening the methyl viologen resistant mutants, the method is as follows: all the mutants seeds and seeds of control T_4-5-4 were sterilized, stratified and then planted on 1/2 MS medium (1.2% Agar, 1.5% sucrose, 1/2 × Murashige-skoog salt, pH=5.7) for vertical growth for10 days. The ten-day-old seedlings were then transferred to 0.20μM methyl viologen additive 1/2MS medium for another growth of 9 days vertically. Those mutants which show longer root growth than the control were selected and concluded as resistant mutants to methyl viologen.

2. 9 Screening methyl viologen resistant *LL729* × Ler F2 mapping population

The method of screening methyl viologen resistant F2 population derived from *LL729* × Ler cross was the same as above-described. Mutant *LL729* and F2 seeds from *LL729* and Ler cross were sterilized, stratified and planted on 1/2 MS medium to grow vertically for 10 days, and then the 10-day-old seedlings were transferred to 0.20μM methyl viologen additive 1/2 MS medium to continue to grow vertically for another 9 days. Those *LL729* × Ler F2 seedlings which displayed longer root growth on 0.20μM methyl viologen additive1/2 MS medium than control, resembling *LL729*, were judged as containing the homozygous mutation loci and picked out for the following positional cloning to identify the mutation gene.

2. 10 Positional cloning to identify the mutation in *LL729*

2. 10. 1 Rough mapping

For the positional cloning of the mutation locus in the mutant *LL729*, we first carried out rough mapping using 30 samples to find out the chromosome arm where the mutation is localized. A series of simple sequence length polymorphism (SSLP) markers

located at different chromosome arms were chosen and used to map the mutation locus. Primers which can amplify the DNA region covering the SSLP markers loci were designed. We used about 30 samples of methyl viologen resistant *LL729* × Ler F2 to do PCR reaction as follows: 94 °C 3min for 1 cycle; 94 °C 20s, 52°C 30s , 72°C 30s for 35 cycles and followed by 72°C extension for 10min. The amplified PCR products were subjected to electrophoresis using a 3% agarose gel and viewed by UV illuminator to determine that the PCR fragments were from homozygous Col-0 or from Col-0/Ler heterozygous DNA at the SSLP loci. The recombination frequency between Ler and Col-0 chromosome during meiosis among the 30 samples of *LL729* × Ler F2 population was counted and used for determining the location of the mutation in the chromosome arm.

2. 10. 2 Fine mapping

After the mutation in the chromosome arm was determined, we used about 400 samples of *LL729* × Ler F2 population for fine mapping. For fine mapping, more denser SSLP markers located in that chromosome arm were chosen and used to narrow down the mutation locus.

2. 11 DNA sequencing of the candidate genes in *LL729* mutant

DNA sequencing of the candidate genes was carried out by using fluorescent-tagged dNTPs as the fluorescent signals for the detection by the DNA sequencing machine. The PCR reaction for the sequencing is: 96°C 1min for 1 cycle, followed by 96°C 10s, 50°C 5s and 60°C 4min for 35 cycles. The PCR products were subjected to the capillary electrophoresis overnight on the DNA sequencing machine ABI3730.

2. 12 Complementation of luciferase imaging phenotype of *LL729*

For genetic complementation of the LUC imaging phenotype, *LL729*, control and F_1seedsderived from*LL729* crossed with a T-DNA mutant (GT_3_3436) which has the T-DNA insertion in the *At5g05630* gene were sterilized and planted on 1/2 MS medium for growing seven days. The luciferase imaging of these seedlings was carried out by using the CCD camera stated above.

2. 13 Heat stress treatment

3-week-old *LL729* and control seedlings growing on 1/2 MS medium (0.5% agar, 1.5% sucrose, half strength Murashige-skoog salt, pH=5.7) were subjected to heat stress treatment as follows: the plates were put in an incubator at 45°C for treatment of 2h, and 2h 20min, respectively. After the heat treatment, the plates were transferred to the growth shelf for recovery at 22°C for another 9 days before taking the pictures. The growth phenotype of the mutant or control after heat treatment was observed and used for judging the thermotolerant or thermosenstive properties of *LL729* and control.

2. 14 Other abiotic stress treatment

2. 14. 1 Cold stress treatment

LL729 mutant and control were stratified and grown on 1/2 MS medium for 7 days. The plates are then put at the refrigerator (4°C) for treatment of 12 hours and then recover at room temperature for another 20min to enhance the translations of transcripts luciferase gene. Then 1mM D-luciferin was sprayed on the seedlings and luciferase imaging was used to detect the intensity of bioluminescence emitted from the seedlings.

2. 14. 2 Salt stress treatment

Seven-day-old *LL729* and control seedlings growing on 1/2 MS medium were pulled out and transferred to a filter paper soaked with liquid 1/2 MS medium plus 100 mM NaCl or 200mM NaCl in a plate for treatment for 16 hours. Then 1mM luciferin was sprayed on the seedlings and luciferase imaging was used to detect the intensity of biolumenscence emitted from the seedlings.

2. 14. 3 Osmotic stress treatment

Seven-day-old *LL729* and control seedlings growing on 1/2 MS medium were transferred to a filter paper soaked with liquid half strength MS medium (pH=5.7) plus

200mM mannitol or 400mM mannitol in a plate, respectively, for treatment of 16 hours. Then 1mM luciferin was sprayed on the seedlings and luciferase imaging was used to detect the intensity of bioluminescence emitted from the seedlings.

Table 2. 1 Markers used for fine mapping to narrow down the mutation loci in mutant *LL729*

Marker name	Primers designed to flank the marker locus	Recombinants
Cer 479329 (T32M21)	5' -CGA AAT CGG AAC CCA CCA-3' 5'-CCA AAT TCG AAA TCA TGG CTG-3'	24/800
Cer 457353 (MUK11)	5'-TCA AGT GAG TTC TTG TTA GCC TAG-3' 5'-GCG GCT ATG TCT TGT GAT CAT C-3'	7/ 800
Cer 457317 (MUG13)	5'-GAA AAT CTA AAC CTT CTC TTG CCG-3' 5'-TGG GAT AAG CAA ATG TAG TCA TGT C-3'	5/800
Cer 454290 (K18I23)	5'-ACG AAA GAA ACC ACT CGG TTC-3' 5'-GAG AGG CTG CTG ATC TTA TTT CC-3'	2/800
Cer 439037 (MOP10)	5' -GCT AGT GGG AGA TAG AGA GAG AGA GG-3' 5'-CTT GCC TCA CAA CAT CCA CC-3'	0/800
Cer 456052 (MJJ3)	5' -ATG GCG TAA TGT TCG TGA AAA G-3' 5'-GAA CCC AAT GAA AAG TCA ATC A-3'	0/800
Cer 434683 (K18J17)	5' -TCA GAC CAT CCT CTC TTC ACT TTC-3' 5'-CTG GTT CCC ATA ATT CTC GAA AG-3'	2/800
Cer 434698 (K18J17)	5'-GTC CCT ATG ATA TGT ATG CCT TTT G-3' 5'-GCA CCA AAA GAG GAA GAC TTT G-3'	3/800
Cer 455774 (MHF15)	5'-CAA CGA TAA CTG ACA AAG TTG TAG C-3' 5'-GCA CAG AAA GGT CAT GAA ACC T-3'	4/800

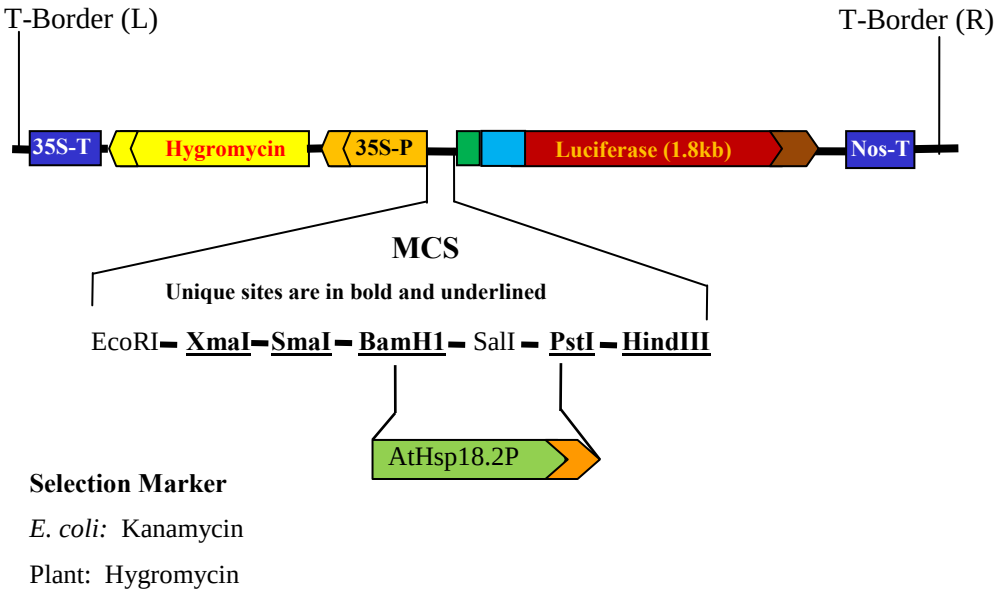

Figure 2. 1 Construction of *At5g59720* promoter-luciferase fusion using pCAMBIA1381-LUC vector.

CHAPTER III
RESULTS

3. 1 *Arabidopsis* transgenic line T_3-5-4 is a homozygous line with a single locus of *T-DNA* insertion

We identified that *Arabidopsis* transgenic line T_3-5-4 is a single locus and homozygous T-DNA transformant based on the genetic segregation of the luciferase imaging phenotype in theT_2 and T_3 generations (Figure 3. 1).

3. 2 Screened *CH*, *HL* and *LL* class mutants

We identified a few of mutants showing constitutively higher luciferase expression (*CH*) at room temperature such as *CH1001* which indicates that *At5g59720* promoter in the *CH* mutants is transcribed constitutively at a higher level even without heat induction. Also, we identified a series of higher luciferase expression mutants (*HL*) after heat induction (i.e, 40°C treatment for 1h) such as *HL307* implying that the transcription of the *At5g59720* promoter-luciferase fusion gene in the *HL* mutants is higher than that in the background after heat induction. Besides, we identified a series of lower luciferase expression mutants (*LL*) such as *LL729* after heat induction (i.e, 40°C treatment for 1h). The luciferase imaging phenotype of these mutants were confirmed in the next generation to make sure that they maintain the same phenotype as their previous generation without and with heat treatment (Figure 3.2).

3. 3 *LL729* is a lower luciferase expression mutant

Based on the luciferase imaging, we found that the luciferase activities in *LL729* mutant were constitutively lower than that in control without heat induction. Besides, after heat induction at 40°C for 1h, the luciferase activities in *LL729* were still lower than that in control T_3-5-4 (Figure 3.3). This indicates that the expression of *At5g59720* promoter-luciferase fusion gene in *LL729* mutant is not as active as that in control.

3. 4 *LL729* mutant is resistant to methyl viologen

Methyl viologen is a toxic compound that can be transported into cytosol of *Arabidopsis* by membrane transporters and is a good electron acceptor which accepts electron transferred from a wide class of electron donors inside the cytosol and it can be also transported into the chloroplast. In the chloroplast, methyl viologen can accept electrons transferred from the Fd (ferrodoxin) on the photo system electron transfer chain and transfer these electrons to substrate like H_2O to produce reactive oxygen species (ROS) such as superoxide radical (O_2^-) and H_2O_2thus blocking the electron transfer chain and generating oxidative stress in *Arabidopsis* (Summers 1980*)*. Based on the root growth assay on the 0.20μM methyl viologen additive 1/2 MS medium, we found that the root growth of *LL729*was about 8 times longer than that in the transgenic background control (Figure 3. 4). Therefore, we concluded that mutant *LL729* is resistant to methyl viologen.

3. 5 *LL729* has no obvious thermotolerant or thermosensitive phenotype

We treated three-week-old seedlings of the *LL729* mutant and T_3-5-4 control line in an incubator at 45°C for 2h and 2h 20mins, respectively. After 9 days recovery at room temperature, the*LL729*mutant did not show obvious thermotolerant or thermosensitive phenotype to heat stress compared with the control line as judged by the growth phenotype after heat treatment (Figure 3. 5).

3. 6 Effects of other abiotic stresses on the induction of *At5g59720* promoter-luciferase fusion gene in the mutant *LL729* and the control line

3. 6. 1 Cold stress treatments on the induction of *At5g59720* promoter-luciferase transgene

The luciferase expression driven by the *At5g59720* promoter in the *Arabidopsis* transgenic background line T_3-5-4 was slightly induced by cold treatment at 4°C in dark for 12 hours. We also observed that *At5g59720* promoter-luciferase transgene in the

mutant *LL729* was slightly induced by cold treatment in dark for 12hours as viewed from the luciferase imaging (Figure 3. 6)

3. 6. 2 Salt stress treatments on the induction of *At5g59720* promoter-luciferase transgene

The induction of *At5g59720* promoter-luciferase fusion gene expression in the T_3-5-4 background line was slightly induced based on my experimental results after salt stress treatment for 16 hours posed by 100mM or 200mM NaCl, respectively (Figure 3. 6). Whereas, the luciferase expression in the mutant *LL729* could not be induced based on the view from the luciferase imaging pictures (Figure 3. 6).

3. 6. 3 Osmotic stress treatments on the induction of *At5g59720* promoter-luciferase transgene

Luciferase expression in the background line T_3-5-4 was slightly induced by osmotic stress treatment for 16 hours with 200mM or 400mM mannitol based on my results, respectively. Whereas, luciferase expression in the mutant *LL729* could not be induced as viewed from the luciferase imaging (Figure 3. 6)

3. 7 Mutation in *LL729* is localized in the gene *At5g05630*

3. 7. 1 Screen the methyl viologen resistant *LL729* × Ler F2 population

Based on the root growth assay on 0.20μM methyl viologen additive 1/2 MS medium, we selected about 400 methyl viologen resistant seedlings from *LL729* × Ler F2 population. These seedlings were used for mapping of the mutated gene locus.

3. 7. 2 Rough mapping

The rough mapping using about 30 samples of F2 methyl viologen resistant seedlings selected from *LL729* and Ler cross revealed that the recombinant frequency between Ler and Col-0 chromosome in the chromosome 5 upper arm is the lowest, whereas the recombinant frequency in other chromosome arms ranged from 40%~60%.

Therefore, we concluded that the *LL729*mutation is located at the chromosome 5 upper arm region.

3. 7. 3 Fine mapping

We used about 400 samples of *LL729* × Ler F2 population for fine mapping. More simple sequence length polymorphism (SSLP) and single nucleotide polymorphism (SNP) markers from the chromosome 5 upper arm were chosen and used to narrow down the mutation locus. The markers used for fine mapping are listed in Table 3. 1. Based on the recombination frequency at each marker's loci, we concluded that the *LL729* mutation is located between the SNP marker Cer434683 in the BAC K18I23 at the chromosome position1768.101kbp and the SSLP marker Cer454290 in the BAC K18J17 at the chromosome position 1576.919 kbp (Figure 3. 7) in the upper arm of the chromosome 5. Each marker has 2 and 2 Ler/Col-0 recombinants, respectively, among all the 400 F_2 samples.

3. 7. 4 DNA sequencing of candidate genes

We chose a few candidate genes located between these two markers (Cer434683 and Cer454290) and sequenced these candidate genes by DNA sequencing. We found that the mutated nucleotide in *LL729* is located in the gene *At5g05630* which encodes a polyamine uptake transporter 3 (PUT3) and the mutant of this gene is called *rmv1*(resistant to methyl viologen). EMS mutagenesis causes a guanine to adenine nucleotide base change at the 755^{th} position of *At5g05630*'s coding sequence (Figure 3. 8). The guanine to adenine nucleotide base change leads to an amino acid substitution of a serine to asparagine at the 252^{th} position of PUT3.

3. 8 PUT3 transmembrane domain prediction

PUT3 is a plasma membrane protein. It belongs to amino acid-polyamine-organocation (APC) superfamily in *Arabidopsis*. The structure of PUT3 is unknown yet, but the transmembrane domains and extracellular and intracellular loops can be predicted by software. Through software prediction by TMHMM

(http://www.cbs.dtu.dk/services/TMHMM) and presented by TMRP2D (http://bioinformatics.biol.uoa.gr/TMRPres2D), we found that PUT3 membrane protein contains 12 transmembrane domains (Figure 3.9). The serine residue at 252th position in wild type PUT3 is localized at cytosolic loop connecting two transmembrane domains TM5 and TM6 based on the TMHMM prediction (Figure 3. 9). The prediction of PUT3 tertiary structure is shown in Figure 3. 10. In the mutant *LL729*, the 252th amino acid residue serine is changed to asparagine and this change is supposed to render the mutant *LL729* resistant to methyl viologen. PUT3 can transport polyamine and its analog methyl viologen but with different affinities, the kinetics parameters for PUT3 transporterare: K_m=0.6 µM for spermine; K_m=2.2 µM for spermidine; K_m=56.5 µM for putrescine and K_m=24.4 µM for paraquat (Shinozaki, K et al., 2012).

3. 9 Exogenous polyamines increase luciferase expression in the mutant *LL729* at normal growth conditions

Without heat induction, after we sprayed higher concentration of spermidine or spermine (10mM, pH=8) on seven-day-old seedlings of the mutant *LL729* and the background line for treatment for 3 hours, we measured the luciferase activity in the seedlings of both *LL729* and background line by using luciferase Imaging. Based on the bioluminescence counts from the luciferase imaging, we found that higher concentration of spermidine and spermine increased luciferase expression in both *LL729* and the background line. The bioluminescent maximum counts increased from the original ~1000 to 2000~5000 for both mutant *LL729* and background line after spraying with spermidine or spermine (Figure 3. 11). These results indicate that exogenous polyamines could rescue the lower luciferase expression phenotype of *LL729*, perhaps via transport of exogenously applied polyamines into the cytosol of *LL729* mutant cells, thus compensating for the cytosolic polyamine concentration that is reduced due to the mutation in the PUT3 in *LL729* mutant.

3. 10 Exogenous polyamines do not increase luciferase expression in the mutant *LL729* after heat induction

When we put the same plate sprayed with spermidine or spermine for 3 hours onto the seedlings to an incubator to treat at 40°C for 1h and took the luciferase imaging again, we found that luciferase activity does not increase as much as that without heat induction (Figure 3. 11). The reason might be that heat activates the transporting activity of polyamine uptake transporters or activate other yet unknown routes of polyamine uptake. It is known that polyamines uptake is temperature dependent (Robert et al., 1991, Morgan et al., 1997). Therefore, a large amounts of spermidine or spermine are transported into the intracellular region of *LL729* mutant after heat treatment and these higher concentration of polyamines bind with the luciferase mRNA in the cytosol to increase its degradation by recruiting the degradosome, therefore, the luciferase activities are reduced in contrast.

3. 11 Complementation of *LL729* luciferase imaging phenotype

In order to confirm that the luciferase imaging phenotype of *LL729* is due to the mutation of gene *At5g05630*, we crossed *LL729* with another *T-DNA* mutant line G_3_3436 which has a T-DNA insertion in *At5g05630*. The F_1 seeds resulted from the genetic cross were planted on 1/2MS medium along with the seeds of *LL729* mutant and T_3-5-4. Luciferase imaging of one-week-old seedlings showed that the luciferase activity in*LL729* × G_3_3436 F1 seedlings was lower than that in the background line T_3-5-4 but resembled the *LL729* mutant (Figure 3.12) at room temperature and after heat stress treatment.This result indicates that G_3_3436 T-DNA line can complement the luciferase imaging phenotype of the mutant *LL729*.

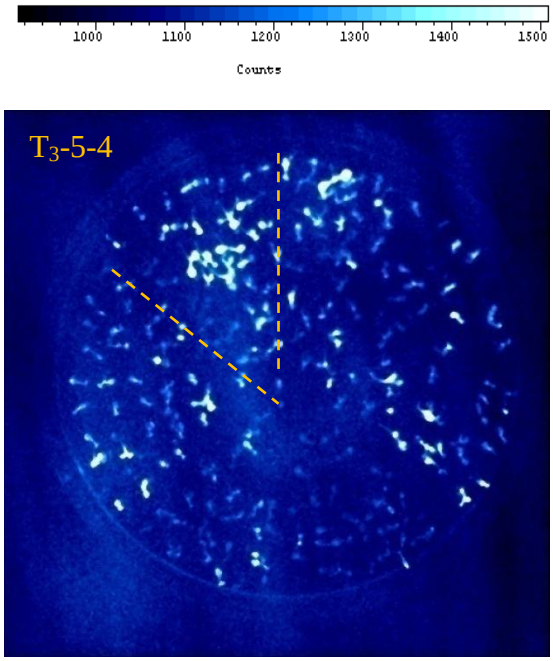

(A)

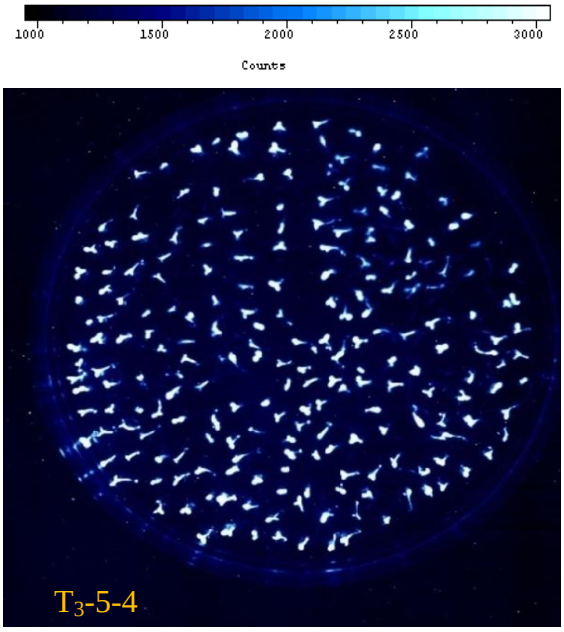

(B)

Figure 3. 1 Confirmation of single locus and homozygous T-DNA transgenic line T_3-5-4 by luciferase imaging. After heat induction at 38°C for 1h, **(A)** using 30 samples, threshold =1500 counts and **(B)** large population, threshold =3000 counts.

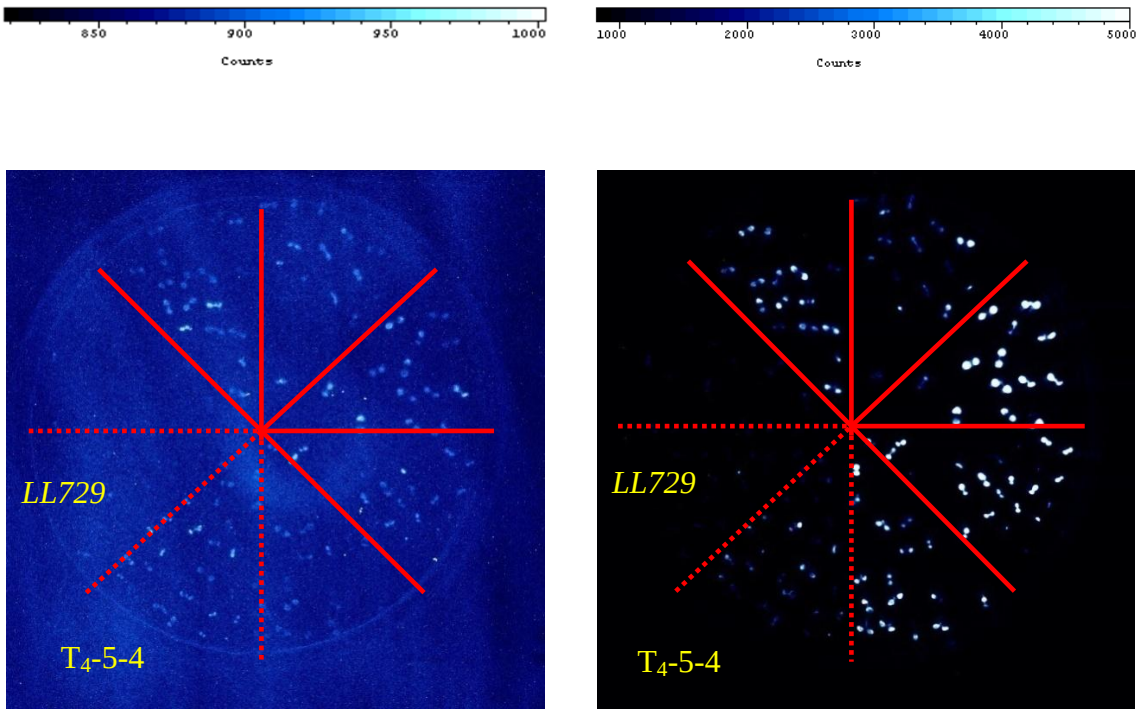

(A) **(B)**

Figure 3. 2 Confirmation of *LL729* mutant phenotype in the second generation. **(A)** Without heat induction, threshold counts=1000, **(B)** after heat induction at 40°C for 30min, threshold counts=5000 by luciferase imaging.

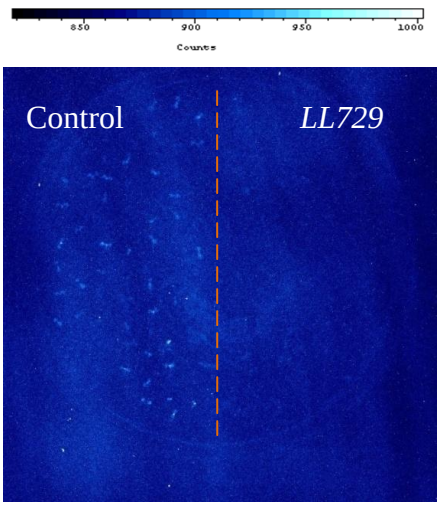

(A)

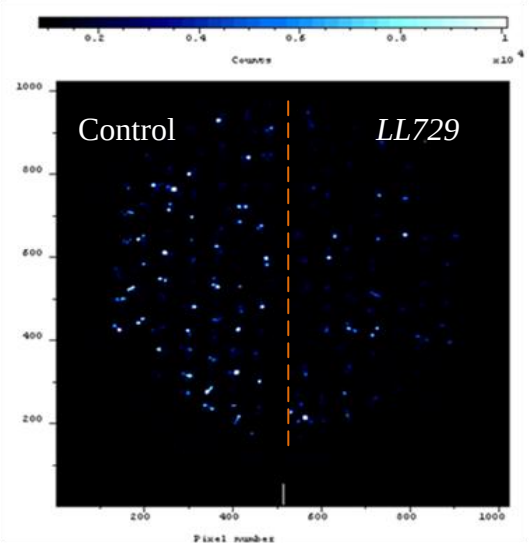

(B)

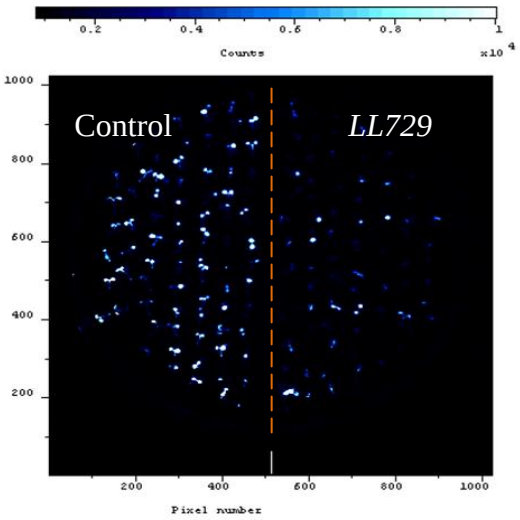

(C)

Figure 3. 3 Luciferse imaging phenotype of *LL729*. **(A)** At room temperautre, threshold=1000 counts, **(B)** 40°C treatment for 1h, threshold=10000 counts, **(C)** 40°C treatment for 1h and 22°C recover for 30min, threshold=10000 counts.

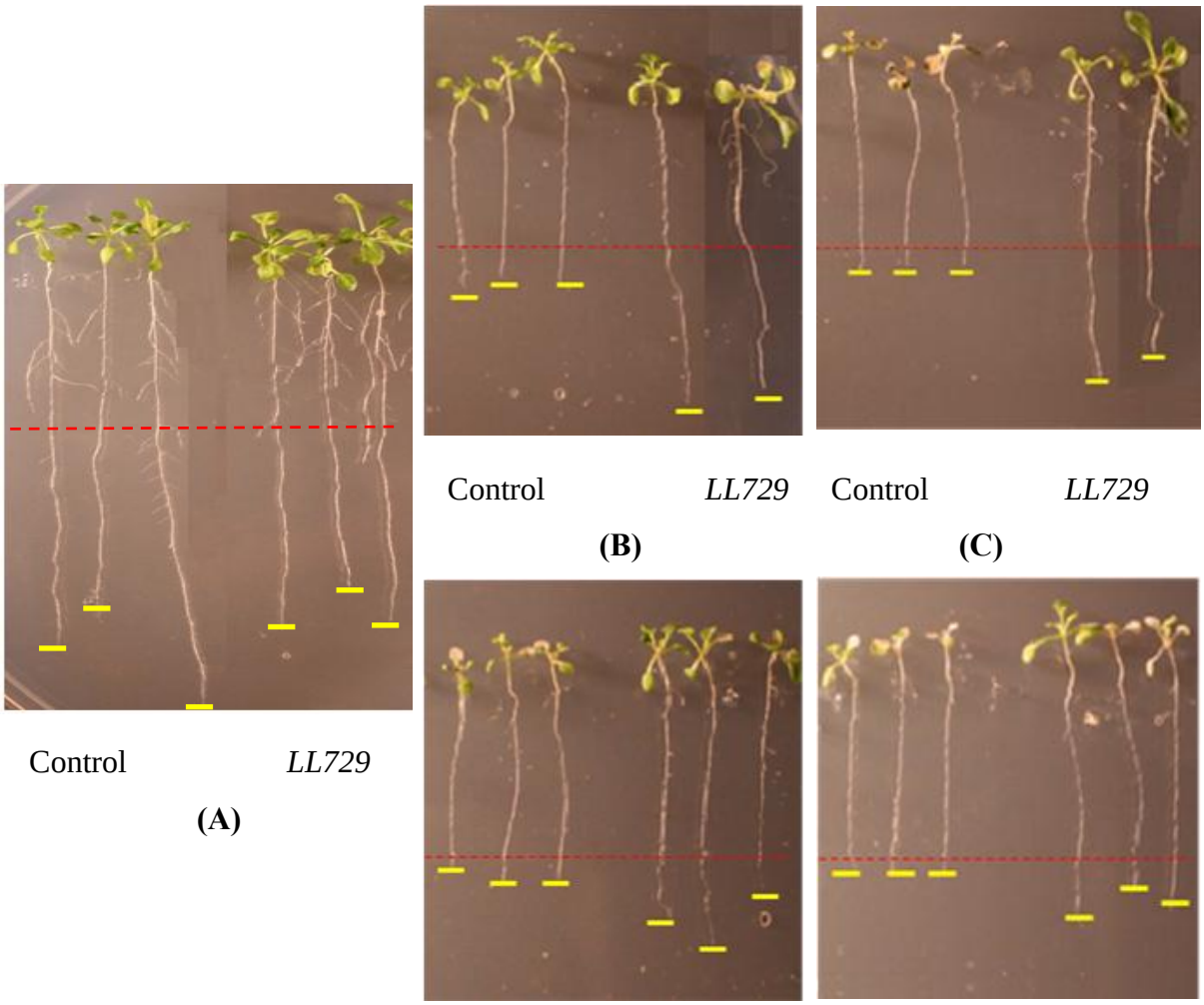

Figure 3. 4 Methyl viologen resistant phenotype of *LL729*. **(A)** 0.00 μM methyl viologen, **(B)** 0.10μM methyl viologen, **(C)** 0.20μM methyl viologen, **(D)** 0.30μM methyl viologen, **(E)** 0.40μM methyl viologen, **(F)** Quantification of root growth of T_3-5-4 and *LL729* on 1/2 MS medium supplemented with methyl viologen

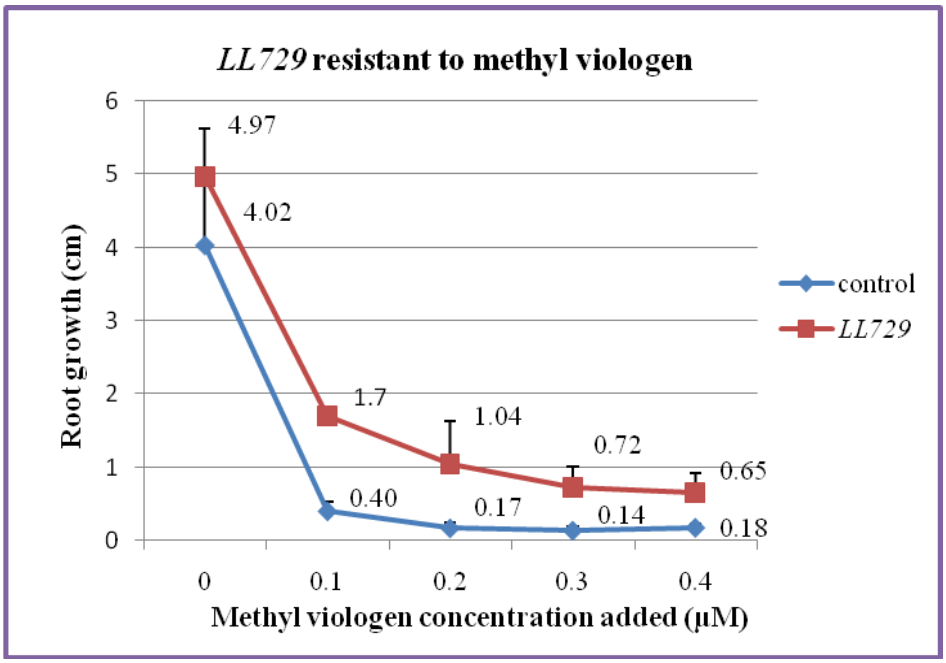

(F)

Figure 3 .4 Continued.

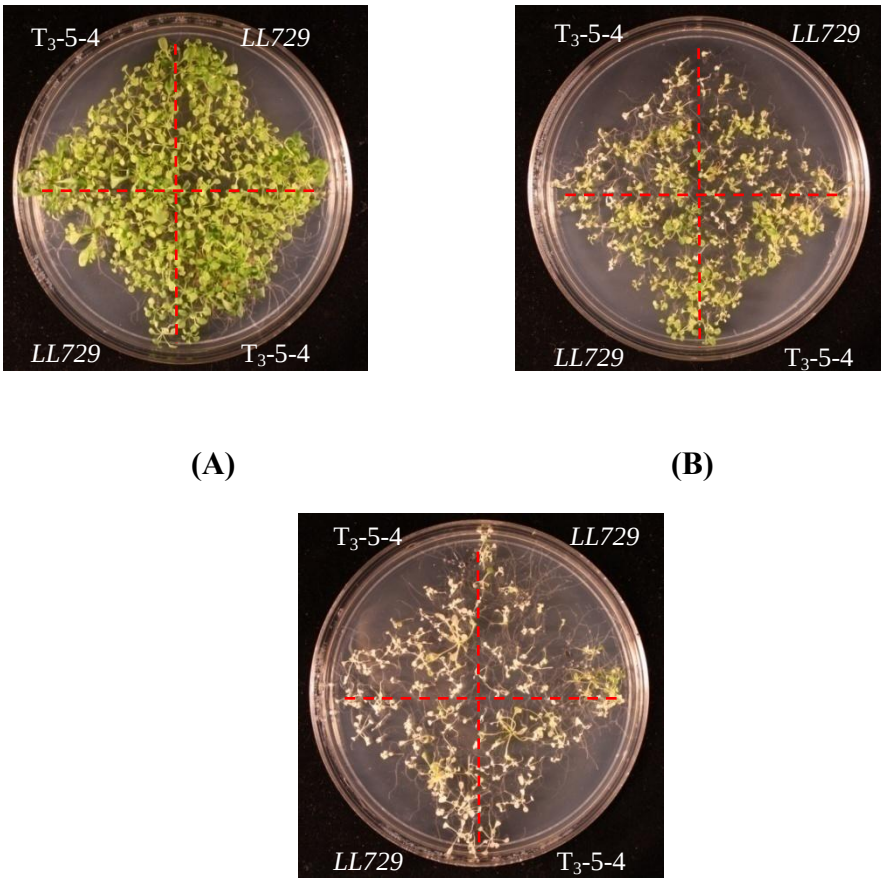

Figure 3. 5 Phenotype of *LL729* after heat stress treatment. **(A)** Control, **(B)** 45°C treatment for 2h and recover at 22°C for 9 days, **(C)** 45°C treatment for 2h 20min and recover at 22°C for 9 days.

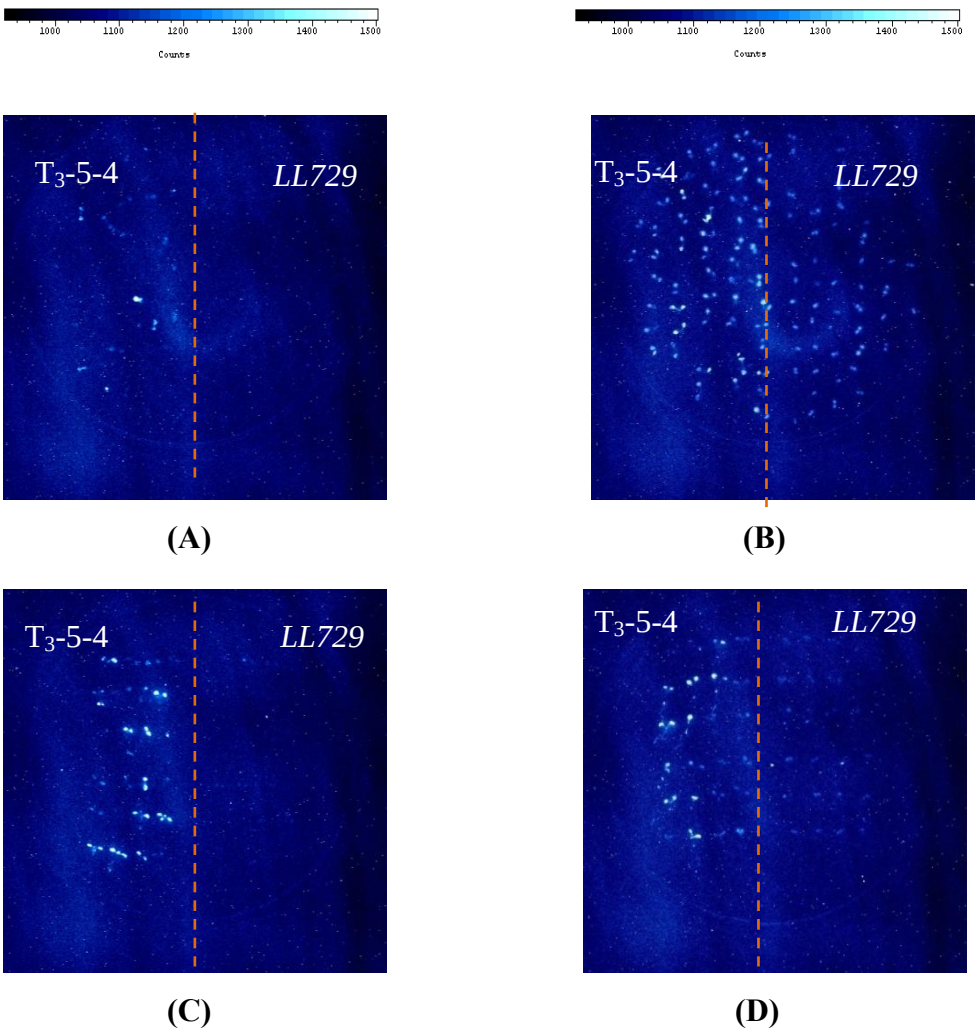

Figure 3. 6 Abiotic stress treatment of the background line T_3-5-4 and *LL729*. **(A)** Control plate without abiotic stress treatment, **(B)** cold treatment for 12h, **(C)** 100mM salt treatment stress treatment for 16h, **(D)** 200mM salt stress treatment for 16h, **(E)** 200mM osmotic stress treatment for 16h, **(F)** 400mM osmotic stress treatment for 16h, intensity of threshold counts for all the luciferase imaging pictures are T=1500.**(G)** Abiotic stresses treatment on the effect of luciferase expression. The average of total counts of photos is by measuring 10 seedlings from the *LL729* and the control in each treatment, respectively. The total counts representing each seedling's area are taken from a region size of 50 × 50 pixels which cover one seeding.

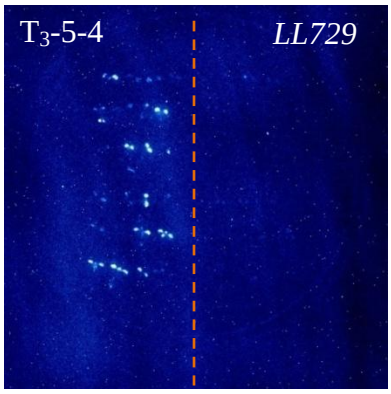

(E)

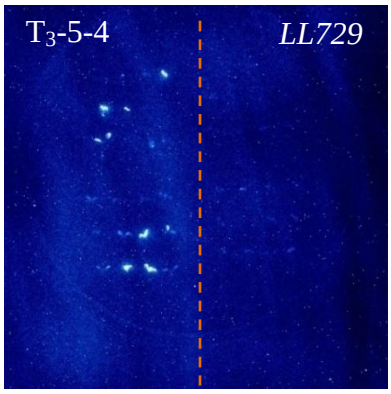

(F)

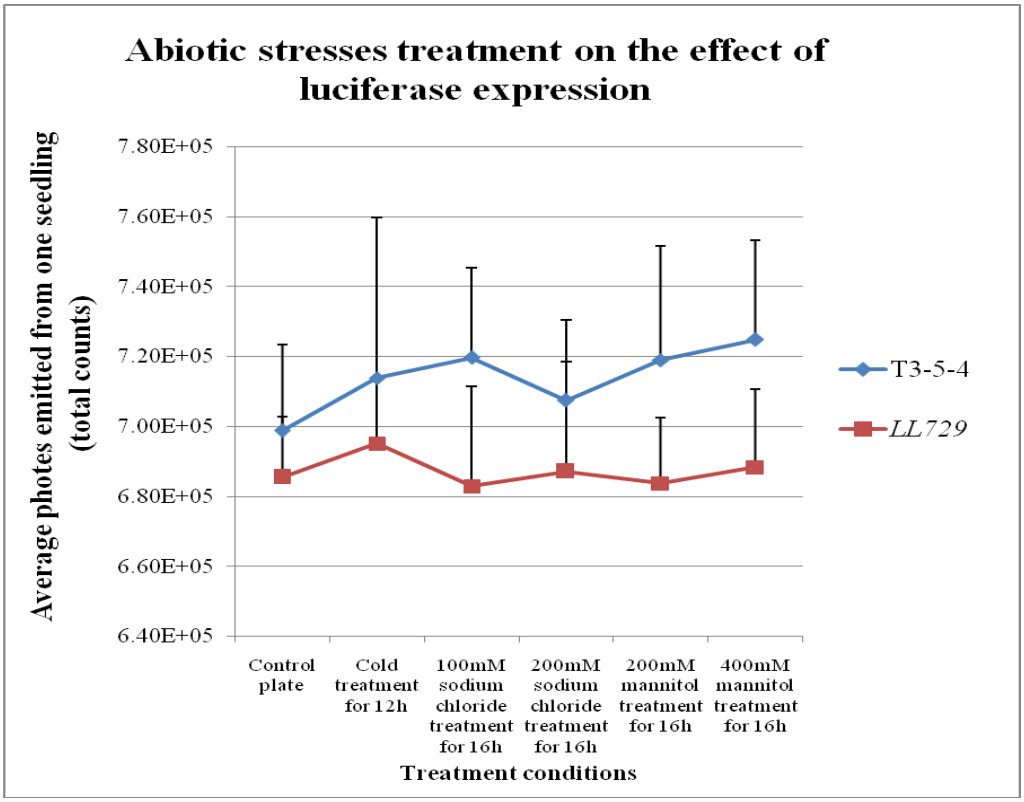

(G)

Figure 3. 6 Continued.

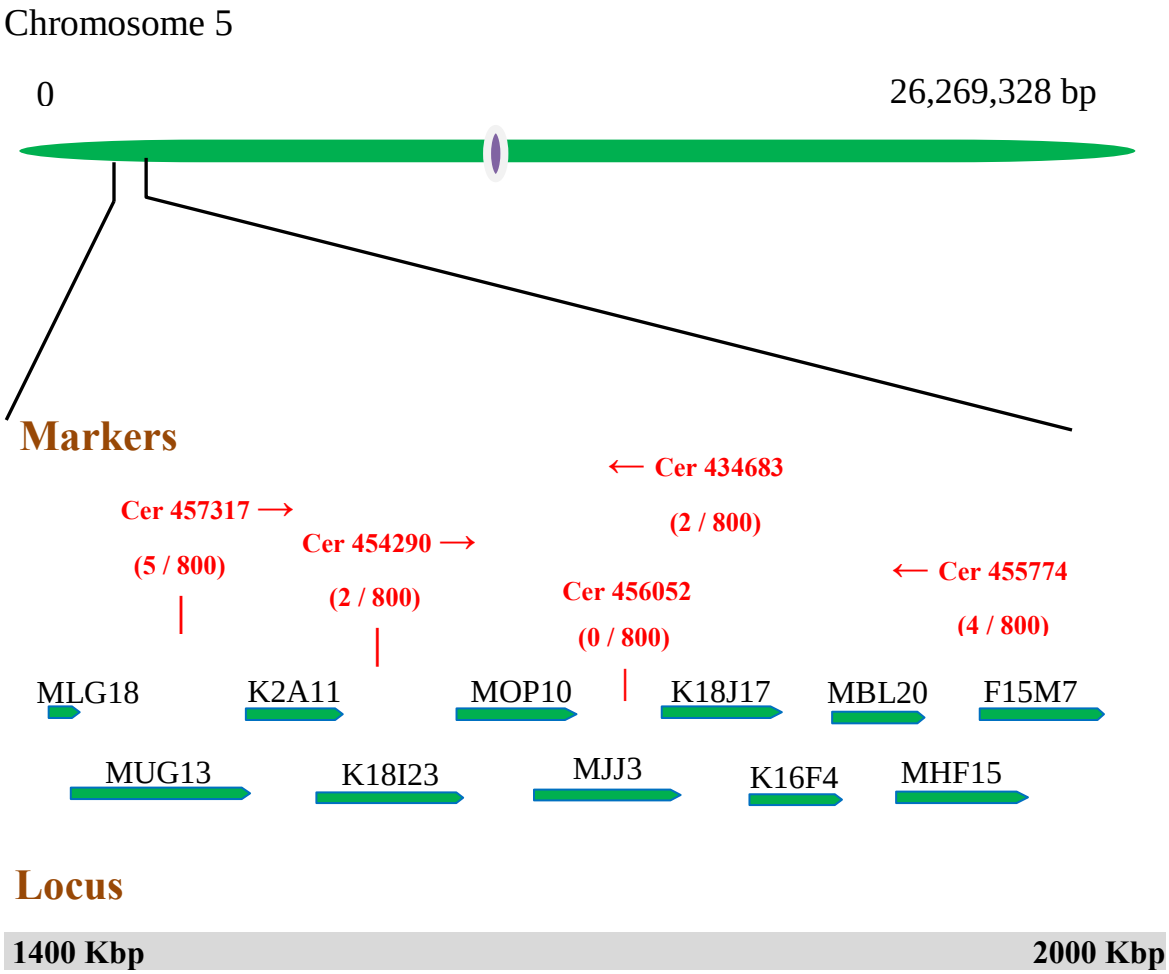

Figure 3. 7 Chromosomal walking to identify the mutation locus in *LL729*.

Primary structure of polyamine uptake transporter 3

1_MTELSSPNLDSASQKPRISTENPPPPPPHISIGVTTGDPATSPARTVN
QIKKITVLPLVFLIFYEVSGGPFGIEDSVKAAGPLLAIVGFIVFPFIWSI
PEALITAEMGTMFPENGGYVVWVTLAMGPYWGFQQGWVKWLSG
VIDNALYPILFLDYLKSGIPILGSGIPRVAAILVLTVALTYLNYRGLSI
VGVAAVLLGVFSILPFVVMSFMSIPKLKPSRWLVVSKKMKGVNWSL
YLNTLFWNLNYWDSV(S/N)TLTGEVENPSKTLPRALFYALLLVVFSY
IFPVLTGTGAIALDQKLWTDGYFADIGKVIGGVWLGWWIQAAAATS
NMGMFLAEMSSDSFQLLGMAERGMLPEVFAKRSRYRTPWVGILFS
ASGVIILSWLSFQEIVAAENLLYCFGMVLEFITFVRLRMKYPAASRPF
KIPVGVLGSVLMCIPPTVLIGVIMAFTNLKVALVSLAAIVIGLVLQPC
LKQVEKKGWLKFSTSSHLPNLME_490

[α]Shaded region indicates the transmembrane domain sequence in PUT3.

(A)

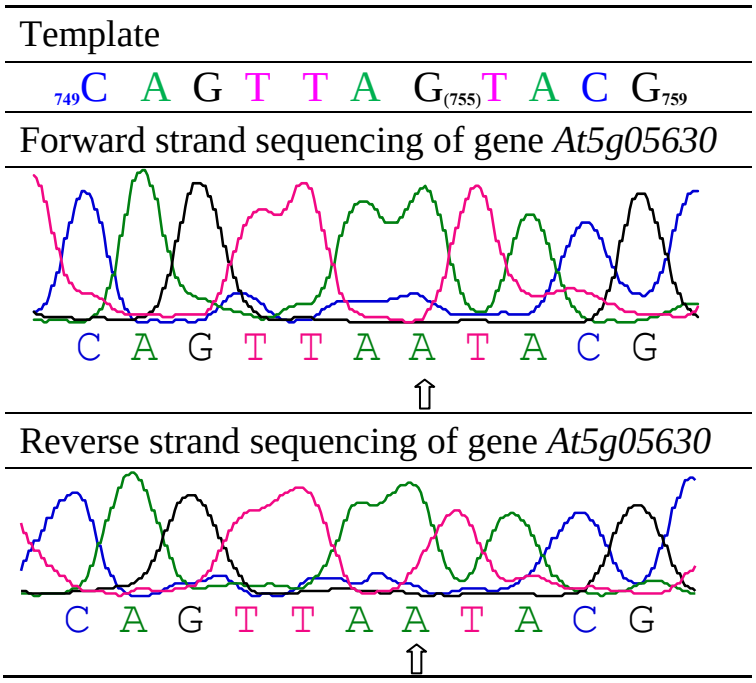

(B)

Figure 3. 8 Amino acid sequence of PUT3 and the DNA sequencing result of gene *At5g05630*. **(A)** Amino acid sequence of PUT3. **(B)** DNA sequencing result of gene *At5g05630***.**

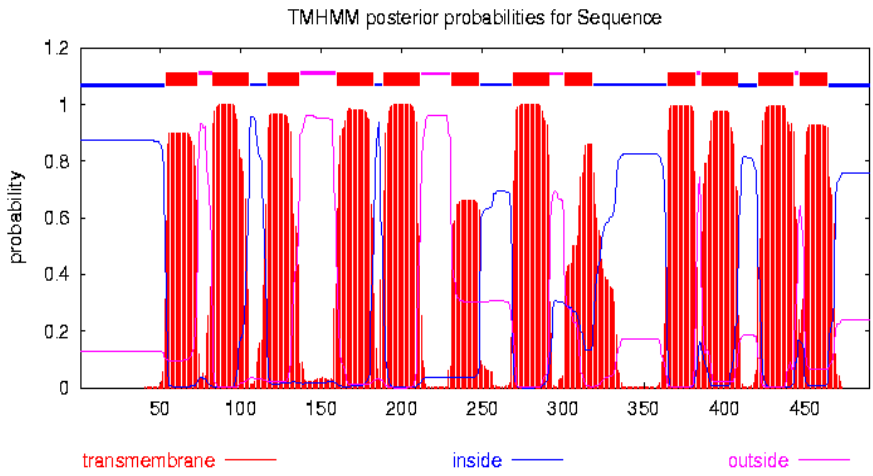

(A)

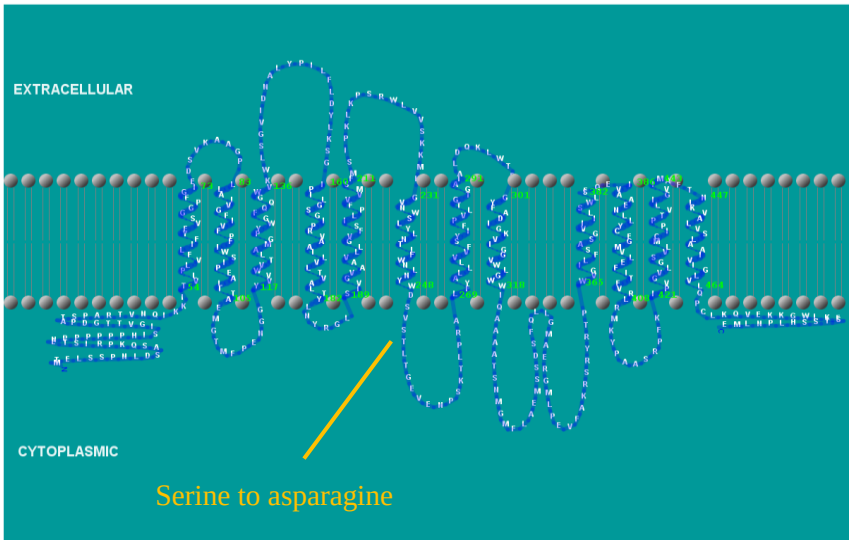

(B)

Figure 3. 9 TMHMM prediction of PUT3 transmembrane helical domains and representation by TMRPres2D.

(A) TMHMM posterior probability of each amino acid predicted by TMHMM software based on the hidden markov model (http://www.cbs.dtu.dk/services/TMHMM/, Krogh et al., 2001). **(B)** TMRPres2D representation of twelve PUT3 transmembrane helical domains, intracellular and extracellular loops (http://bioinformatics.biol.uoa.gr/TMRPres2D/, Spyropoulos et al., 2004).

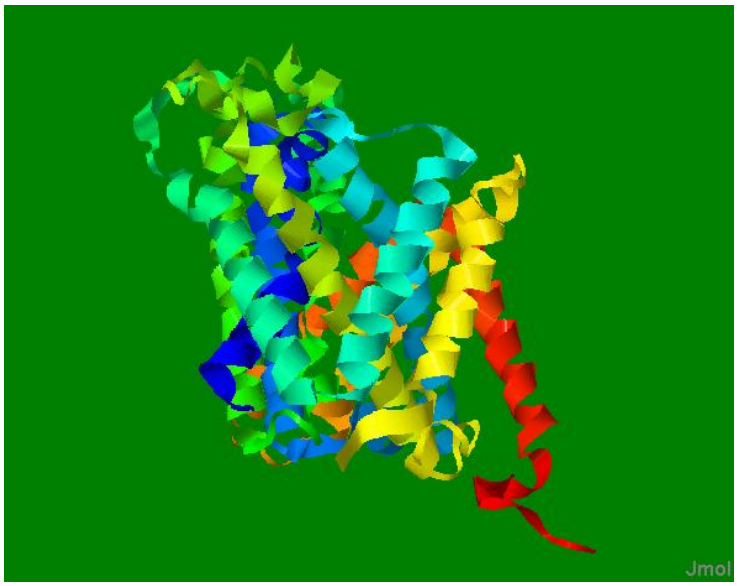

Figure 3. 10 Predicted tertiary structure of PUT3 by FFAS03 based on template 3ncy. The prediction is based on the profile – profile comparsion which scans the protein structure database. The template is a knownarginine agmatine antiporter protein with entry of 3ncy.pdb in protein data bank. The link for the prediction website is http://ffas.ljcrf.edu/ffas-cgi/cgi/ffas.pl (Schwarzenbacher et al., 2008).

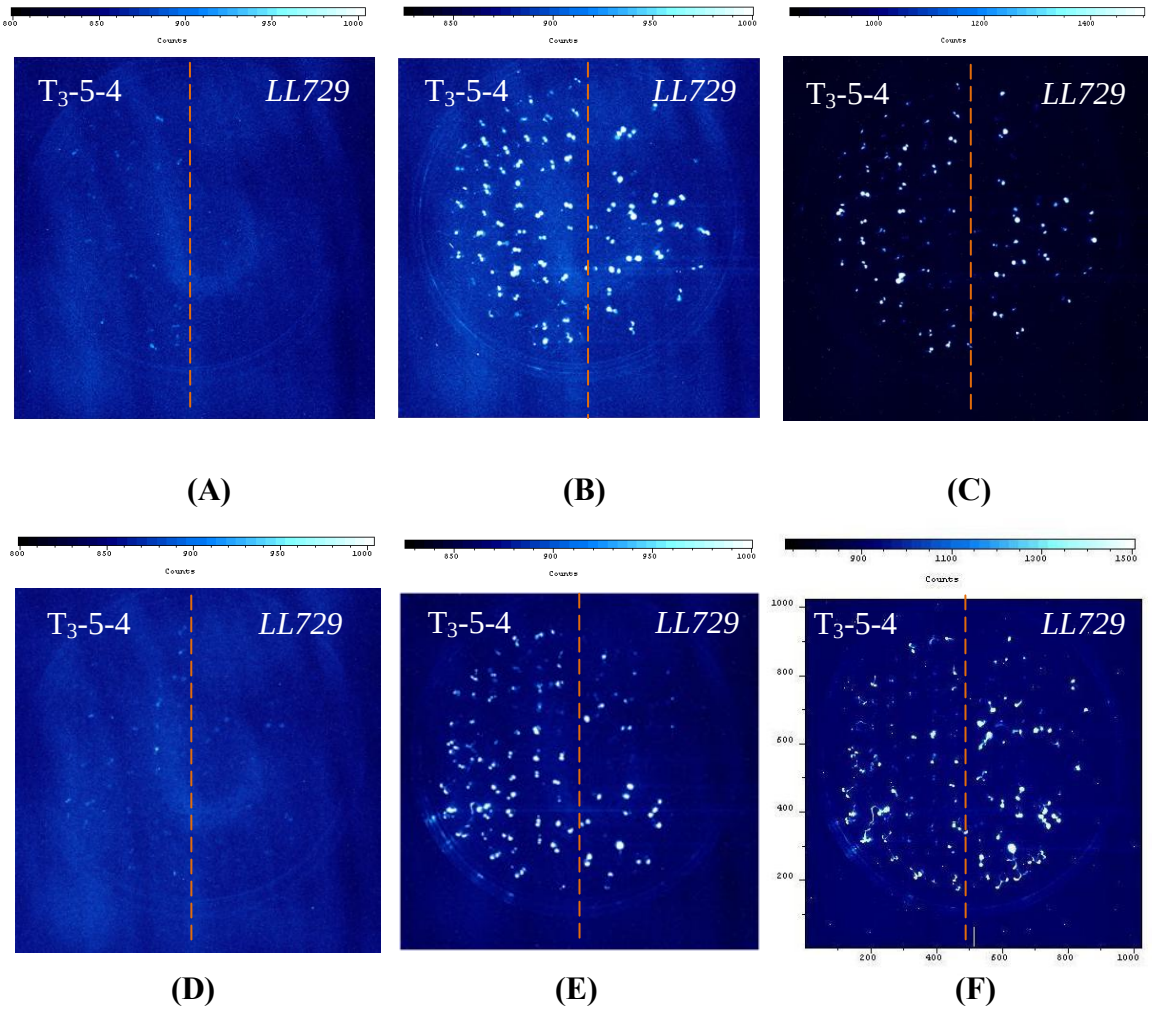

Figure 3. 11 Polyamines affect the luciferase activities in *LL729* and the background line T_3-5-4. **(A)** Control plate 1, **(B)** spraying 10mM spermine for 3 h, **(C)** spraying 10 mM spermine for 3h and 40°C treatment for 1h, **(D)** control plate 2, **(E)** spraying 10mM spermidine for 3h, **(F)** spraying 10mM spermidine for 3h and 40°C treatment for 1h. The threshold intensity for imaging pictures **(A)**, **(B)**, **(D)**, **(E)** are T=1000, and the threshold intensity for **(C)** and **(F)** are T=1500 as shown in the intensity bar. **(G)** Quantification of photos emitted fron each *LL729* and control seedling after spermine treatment. **(H)** Quantification of photosemitted fromeach *LL729* and control seedling after spermidine treatment. The quantification is bycounting 10 seedlings and substract the average background counts within a size of 2280 pixels from the the total counts of a region size of 50 × 50 pixels which contain both the counts of the background and the seedling.

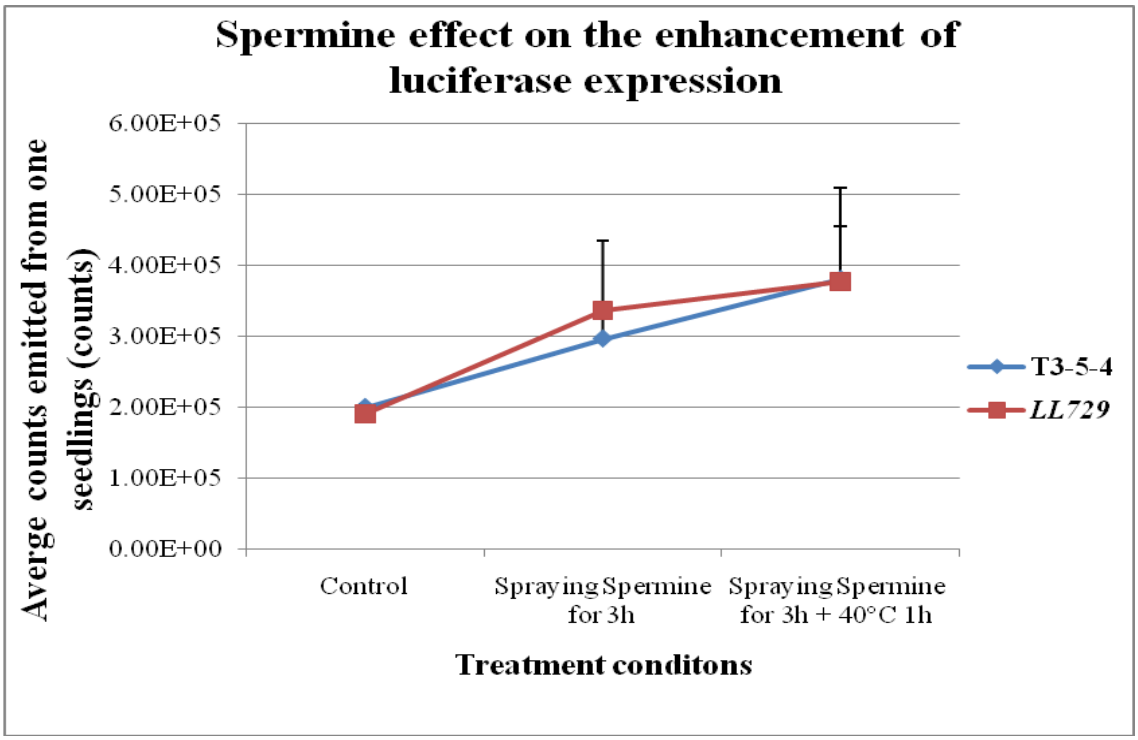

(G)

Figure 3. 11 Continued.

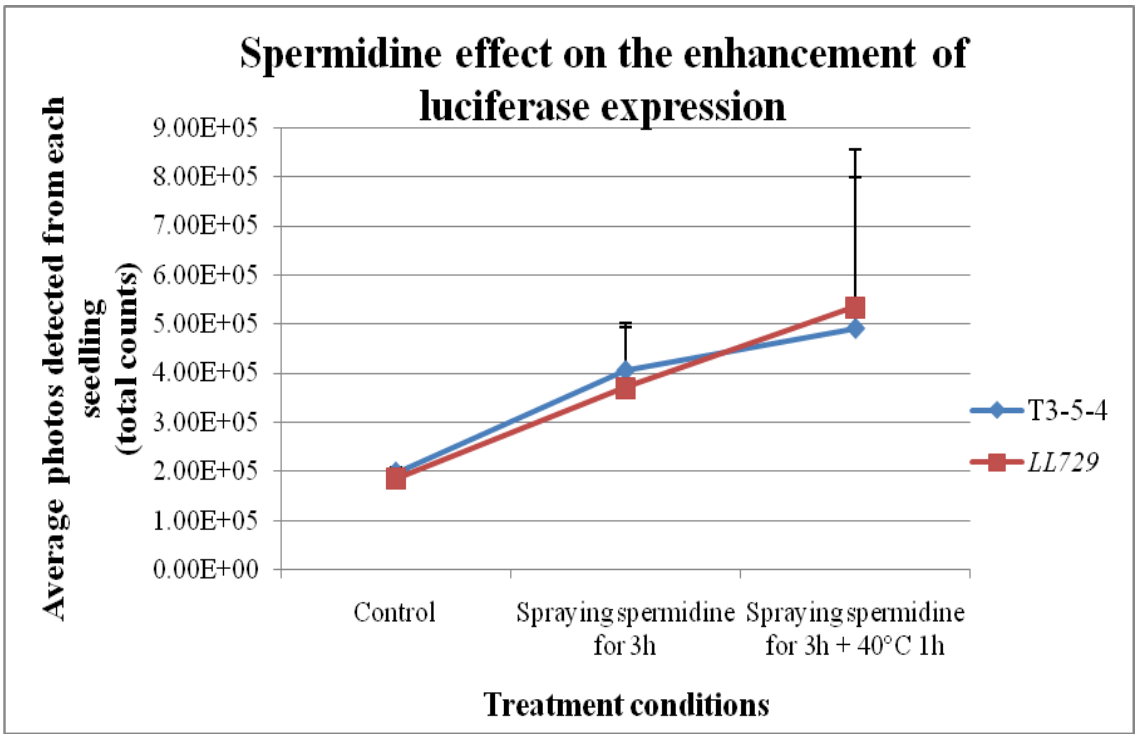

(H)

Figure 3. 11 Continued.

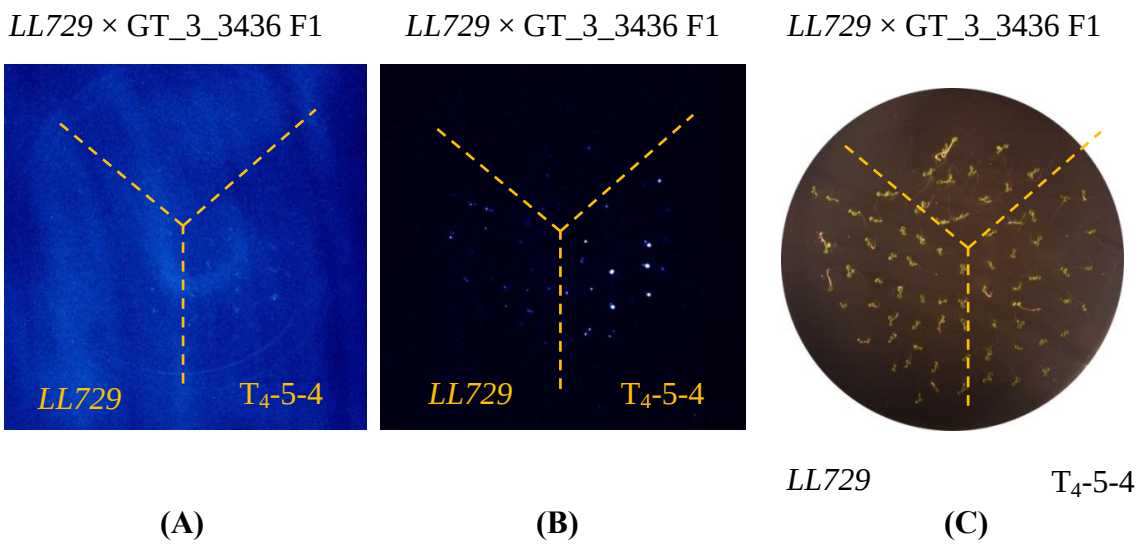

Figure 3. 12 Complementation of *LL729* luciferase imaging phenotype. **(A)** Without heat induction, threshold counts=1300. **(B)** Heat induction at 40°C for 1h, threshold counts=2000. **(C)** Seven-day-old seedlings before treatment.

CHAPTER 4
CONCLUSIONS AND DISCUSSIONS

4. 1 Mutation of Ser_{252} to Asn_{252} in PUT3 affects its transporting activity in *LL729* and renders it resistant to methyl viologen

In mutant *LL729*, the nucleotide mutation from guanine to adenine in the gene *At5g05630* leads to a serine to asparagines change at the 252th position of PUT3, which is located at the cytosolic loop region connecting two transmembrane domains of TM 5 and TM 6 in PUT3 (Figure 3. 9). The amino acid substitution at this position is predicted to have the following possible effects on the normal functions of PUT3: i) the mutation could affect PUT3's normal folding and assembly into the plasma membrane thus affecting its normal function. ii) $serine_{252}$ might be a potential phosphorylation site, $serine_{252}$ to $asparagine_{252}$ mutation may lead to the loss of PUT3's post translational modification such as phosphorylation by certain protein kinases at the $serine_{252}$ site which will affect the regulation of the membrane protein, therefore the mutation inhibits the membrane protein's function. iii) $serine_{252}$ to $asparagine_{252}$ mutation might affect the binding or targeting of $serine_{252}$ residue by other activators or regulators which furthermore affects the regulation of the channel thus affecting its function of transporting extracellular substances. These possible effects of the mutation on PUT3's functions are needed to be further verified by experiments. It was found that another amino acid substitution at 377th site from isoleucine **(I)** to phenylalanine **(F)** in PUT3 of *Arabidopsis* ecotopye Nos-d leads it to be resistant to methyl viologen toxicity; this amino acid change is located at the transmembrane domain and is supposed to directly affect the membrane protein folding on the plasma membrane thus affecting its function of the transporter (Shinozaki et al., 2012).

4. 2 Mutation of Ser_{252} to Asn_{252} in PUT3 affects its transporting activity of polyamines in *LL729*

Shinozaki et al (2012) used transporter assay and found that, Ile_{377} to Phe_{377} substitution not only reduce the transportation of substrate like methyl viologen, but also reduce the transportation of putresince, spermidine and spermine into cytosol by using radioactive labeling polyamines. It was proposed that Ile is essential for the folding of the protein. Besides, the transportation of polyamines by PUT3 can be affected by pH (Shinozaki et al., 2012).

We treated the *LL729* mutant with high concentration of polyamines and found that exogenous polyamines can enhance the luciferase activities. We think increasing the polyamine concentration from the environment could increase the transportation of polyamine into the cytosol. Besides, we supposed that there are other possible polyamine uptake transporters that may play a role in transporting polyamines at higher polyamine concentrations. Therefore, when higher concentration of polyamines is present extracellularly, these low affinity transporters can transport polyamines into the cytosol, thus compensating for the loss-of-function of PUT3 in the *LL729* mutant. Data from Shinozaki et al (2012) also imply that, in addition to PUT3, there are other possible polyamines transporters for polyamine influx. There are five known homologs of PUTs in *Arabidopsis* (Figure 4. 1) and none of their crystal structures are known; they share very high identity in protein sequences (See Table 4. 1). The tertiary structure prediction of PUT3 based on the homology is shown in Figure 3. 10.

We hypothesize that Ser_{252} to Asn_{252} mutation in PUT3 not only reduces the transportation of substrates like methyl viologen into cytosol which renders *LL729* resistant to methyl viologen but also reduces the transportation of polyamines like putrescine, spermidine and spermine into the cytosol since polyamines carry the same positive charge as methyl viologen in the acidic pH condition (Table 4. 2).

In mutant *LL729*, we found that the expression of luciferase gene driven by the *At5g59720* promoter is lower than that in the background line from the luciferase imaging. We think the reason is because of the content of the intracellular polyamines in *LL729* is less than that in the background line due to the loss of transportation function of PUT3 caused by mutation which eventually affect the basal and induced expression of the luciferase gene. After we sprayed 10mM spermidine or spermine on the leaves of *LL729* and background line to enhance the transportation of spermine or spermidine into the cytosol, we found that *At5g59720* promoter driven luciferase expression were increased based on the increased bioluminescent counts as we expected.

4. 3 Decreased intracellular polyamines reduce basal and induced expressions of heat-inducible genes in *LL729* and the possible mechanisms

Because polyamines such as putrescine, spermidine and spermine carry a positive charge at each amine group and resemble the analog of methyl viologen (Table 4. 2). Inside the cells, polyamines can bind to DNA, RNA or even enzyme non-specifically and affect the formation of their structure and thus their functions. It is known that polyamines are involved widely in the functions of cellular processes, such as gene transcription, translation, nucleotide acid packing, DNA replication and mRNA degradation and so on (Yoshida et al., 1999; Deng et al., 2000; Igarashi et al., 2010).

Polyamines can affect the activities of histone acetyltransferases (HATs) and histone deacetylases (HDATs) which can affect the balance of acetylation status in histones (Iwashita et al., 2011). In eukaryotes, DNA is barely exposed outside and is wrapped around histones in a nucleosome unit to form the chromatin structure. When gene is transcribed actively, the chromatin structure is loose and hisone can be removed by chromatin remodeling complex and transcriptional machine can process the transcription. While gene is not transcribed and the chromatin structure is compacted by the binding complex and the pre-initiation complex cannot be assembled at the TATA box region due to the condensed chromatin structure. Histone proteins include five

normal forms of subunits: H1, H2A, H2B, H3 and H4, however, histones also have isoforms. For instance, H3.3 is an isoform of H3 which has 4 different amino acids (Goll et al., 2002). The amino acids on each N-terminus of H2A, H2B, H3 and H4 histone proteins can be post-translationally modified such as phosphorylation, acetylation, ubiquitilation and methylation at the relative amino acid sites by different enzymes and the differently modified amino acids can be further bound by the relative binding complex (Goll et al., 2002). These arranged specific post-translational modifications of amino acids in the histones are called "histone code" (Berger et al., 2002). Different "histone code" status will be recognized by different binding complex and dictate the gene's transcriptional status. Therefore, the change of "histone code" can regulate the transcription of genes such as enhance or inhibit the transcription as well as turn on or off a gene's expression. Figure 4. 2 shows the different post-translational modifications of amino acids on histone3 and histone 4 in *Arabidopsis*.

It was reported that higher levels of intracellular polyamines could promote histone acetyltransferase that results in hyperacetylation of histones and thus changes the "histone code" staus (Iwashita et al., 2011). Hyperacetylation of histones promotes gene transcription through acetylated lysines on the histone tails acting as a marker to berecognized by the bromodomain of TFIID and chromatin remodeling complex (Agalioti et al., 2002). The acetylated lysine residues such as H3K9ac and H3K14ac can be targeted by the bromodomain of TFIID and therefore recruit TFIID to bind around the TATA region of a gene to start for assembling the pre-initiation complex. Also, acetylated lysines can be recognized and bound by the bromodomain of chromatin remodeling complex to help remove the histone at the promoter and gene's coding region and make the gene accessible by the transcriptional machinery for transcription. For instance, acetylation of lysine 8 in the histone H4 (H4K8ac) at the N-terminal tail mediates the recruitment of the chromatin remodeling complex SWI/SNF while acetylation of lysine 9 and lysine 14 in histone H3 (H3K9ac and H3K14ac) at the N-terminal tail is critical for the recruitment of TFIID (Figure 4. 3) (Agalioti et al., 2002).

Therefore, in the mutant *LL729*, reduced intracellular polyamines content due to the mutation in PUT3 are thought to affect both the basal expression of heat shock gene *At5g59720* without heat stress because of reduced acetylation of lysine residues in the hisones located at the *At5g59720* promoter and encoding sequence which causes the chromatin structure of *At5g59720* gene in a condensed conformation and the RNA transcriptional machinery cannot bind to the *At5g59720* promoter, thus, the transcription is inhibited.

In mutant *LL729*, after heat stress treatment, luciferase transcription driven by the *At5g59720* promoter is increased than that without heat treatment. This is probably due to that activated or induced AtHsfs can still bind to the HSEs in the *At5g59720* promoter after heat treatment to enhance the transcription, but the transcription level of luciferase in *LL729*is still reduced compared with that in the background line after heat treatment. The possible explanation could be that, after heat treatment, although the histones occupancy at *At5g59720* gene is greatly reduced, and the activated AtHsf can bind to HSEs, but the binding efficiency of AtHsf with HSEs is not as good as that in the control because of the reduced polyamines contents in the nucleus reduce the binding efficiency of AtHsfs with HSEs. The reduced binding of AtHsfs with HSEs will also negatively affect H3 acetylation status and H3 occupancy. Therefore, the transcription of luciferase gene is still reduced.

Using electrophoretic mobility shift assay (EMSA), it was reported that polyamines and its precursor glutamine can enhance the binding of Hsf-1 with the heat shock elements located in the Hsp70 and Hsp25 promoters under heat stress (Iwashita et al., 2011), although the detailed mechanism of polyamines enhancing the binding Hsf-1 with HSEs is not very clear. How polyamines enhance the binding of Hsf-1 with the HSEs of Hsp70, Hsp25 and other heat stress inducible genes deserves further study. Questions remain to be answered as to whether enhanced binding of Hsfs with HSEs is through directly or indirectly mediated formation of Hsf-1 and HSE binding complex or through helping bending of the DNA around the promoter region by neutralizing the

negative charge on the phosphate group of DNA to reduce the energy for DNA bending (Feuerstein et al., 1989; Maher 1998).

Table 4. 1 Sequence alignment of polyamine uptake transporter homologs in *Arabidopsis*

```
PUT1_At3g31820      MQKRRIITVNPSASIEMSQYENNE--VPYSSVGAD--EVPSSPPKATDKIRKVSMLPLVF 56
PUT2_At3g31830      MQKRRIITVNPSASIEMSQYENNE--VPYSSVGAD--EVPSSPPKATDKIRKVSMLPLVF 56
PUT3_At5g05630      MTELSSPNLDSASQKPRISTENPPPPPPHISIGVTTGDPATSPARTVNQIKKITVLPLVF 60
PUT5_At1g19553      MGEEETIVNDENSSKP----------------------KPSP--------KLTLLPLVF 29
PUT4_At3g13620      MAISEASKSSHELPVT----------------------TAESSGKKATAKKLTLIPLVF 37
                    *        .                              ...        *:::*****
PUT1_At3g31820      LIFYEVSGGPFGVEDSVNAAG-PLLALLGFVIFPFIWSIPEALITAEMGTMYPENGGYVV 115
PUT2_At3g31830      LIFYEVSGGPFGVEDSVNAAG-PLLALLGFVIFPFIWSIPEALITAEMGTMYPENGGYVV 115
PUT3_At5g05630      LIFYEVSGGPFGIEDSVKAAG-PLLAIVGFIVFPFIWSIPEALITAEMGTMFPENGGYVV 119
PUT5_At1g19553      LIFYEVSGGPFGVEDSVKSGGGPLLALLGFLIFPLIWSIPEALVTAELATSFPENGGYVV 89
PUT4_At3g13620      LIYFEVAGGPFGEEPAVQAAG-PLLAILGFLIFPFIWSIPEALITAELSTAFPGNGGFVI 96
                    **::**:***** * :*::.* ****::**::**:********:***:.* :* ***:*:
PUT1_At3g31820      WVSSALGPFWGFQQGWMKWLSGVIDNALYPVLFLDYLKSGVPALGSGLPRVASILVLTIL 175
PUT2_At3g31830      WVSSALGPFWGFQQGWMKWLSGVIDNALYPVLFLDYLKSGVPALGSGLPRVASILVLTIL 175
PUT3_At5g05630      WVTLAMGPYWGFQQGWVKWLSGVIDNALYPILFLDYLKSGIPILGSGIPRVAAILVLTVA 179
PUT5_At1g19553      WISSAFGPFWGFQEGFWKWFSGVMDNALYPVLFLDYLKHSFPVLDHVAARVPALLVITFS 149
PUT4_At3g13620      WAHRAFGSFVGSMMGSLKFLSGVINVASFPVLCVTYLDKLFPVLESGWPRNVCIFASTVV 156
                    *   *:*.: *   *  *::***:: * :*:* : **.  .* *    .*  .::. *.
PUT1_At3g31820      LTYLNYRGLTIVGWVAVLMGVFSILPFAVMGLISIPQLEPSRWLVMD--LGNVNWNLYLN 233
PUT2_At3g31830      LTYLNYRGLTIVGWVAVLMGVFSILPFAVMGLISIPQLEPSRWLVMD--LGNVNWNLYLN 233
PUT3_At5g05630      LTYLNYRGLSIVGVAAVLLGVFSILPFVVMSFMSIPKLKPSRWLVVSKKMKGVNWSLYLN 239
PUT5_At1g19553      LTYLNYRGLHIVGFSAVVLAVFSLCPFVVMALLAVPNIRPKRWLFVD--TQKINWRGYFN 207
PUT4_At3g13620      LSFLNYTGLAIVGYAAVVLGLVSLSPFLVMSAMAIPKIKPHRWGSLG--TKKKDWNLYFN 214
                    *::*** ** ***  **::.:.*: ** **. :::*::.* **  :.      :*  *:*
PUT1_At3g31820      TLFWNLNYWDSISTLAGEVENPNHTLPKALFYGVILVACSYIFPLLAGIGAIPLERE-KW 292
PUT2_At3g31830      TLFWNLNYWDSISTLAGEVENPNHTLPKALFYGVILVACSYIFPLLAGIGAIPLERE-KW 292
PUT3_At5g05630      TLFWNLNYWDSVSTLTGEVENPSKTLPRALFYALLLVVFSYIFPVLTGTGAIALDQK-LW 298
PUT5_At1g19553      TMFWNLNYWDKASTLAGEVDRPGKTFPKALFGAVLLVMGSYLIPLMAGTGALSSSTSGEW 267
PUT4_At3g13620      TLFWNLNFWDNVSTLAGEVDEPQKTFPLALLIAVIFTCVAYLIPLFAVTGAVSVDQS-RW 273
                    *:*****:**. ***:***:.* :*:* **: .:::.  :*::*:::  **:. . .  *
PUT1_At3g31820      TDGYFSDVAKALGGAWLRWWVQAAAATSNMGMFIAEMSSDSFQLLGMAERGMLPEFFAKR 352
PUT2_At3g31830      TDGYFSDVAKALGGAWLRWWVQAAAATSNMGMFIAEMSSDSFQLLGMAERGMLPEFFAKR 352
PUT3_At5g05630      TDGYFADIGKVIGGVWLGWWIQAAAATSNMGMFLAEMSSDSFQLLGMAERGMLPEVFAKR 358
PUT5_At1g19553      SDGYFAEVGMLIGGVWLKGWIQAAAAMSNLGLFEAEMSSDAFQLLGMSEIGMLPAFFAQR 327
PUT4_At3g13620      ENGFHAEAAEMIAGKWLKIWIEIGAVLSSIGLFEAQLSSSAYQLEGMAELGFLPKFFGVR 333
                     :*:.:: .  :.* **  *:: .*. *.:*:* *::**.::** **:* *:** .*. *
PUT1_At3g31820      SRYG-TPLLGILFSASGVVLLSWLSFQEIVAAENLLYCVGMILEFIAFVRMRMKHPAASR 411
PUT2_At3g31830      SRYG-TPLLGILFSASGVVLLSWLSFQEIVAAENLLYCVGMILEFIAFVRMRMKHPAASR 411
PUT3_At5g05630      SRYR-TPWVGILFSASGVIILSWLSFQEIVAAENLLYCFGMVLEFITFVRLRMKYPAASR 417
PUT5_At1g19553      SKYG-TPTISILCSATGVIFLSWMSFQEIIEFLNFLYALGMLLEFAAFVKLRIKKPDLHR 386
PUT4_At3g13620      SKWFNTPWVGILISALMSLGLSYMNFTDIISSANFLYTLGMFLEFASFIWLRRKLPQLKR 393
                    *::  ** :.** **   : **::.* :*:   *:** .**.*** :*: :* * *   *
PUT1_At3g31820      PYKIPIGTTGSILMCIPPTILICAVVALSSLKVAAVSIVMMIIGFLIHPLLNHMDRKRWV 471
PUT2_At3g31830      PYKIPIGTTGSILMCIPPTILICAVVALSSLKVAAVSIVMMIIGFLIHPLLNHMDRKRWV 471
PUT3_At5g05630      PFKIPVGVLGSVLMCIPPTVLIGVIMAFTNLKVALVSLAAIVIGLVLQPCLKQVEKKGWL 477
PUT5_At1g19553      PYRVPLNTFGVSMLCLPPSLLVILVMVLAAPKTFLISGVIIVLGFCLYPFLTLVKEKQWA 446
PUT4_At3g13620      PYRVPLKIPGLVVMCLIPSAFLVLILVFATKIVYLICGVMTIGAIGWYFLINYFRKTKIF 453
                    *:::*:   *  ::*: *: ::  ::.::    .  :. .  : .:     :. . ..
PUT1_At3g31820      KFS---------ISSDLPDLQQQTREYEETLIR 495
PUT2_At3g31830      KFS---------ISSDLPDLQQQTREYEETLIR 495
PUT3_At5g05630      KFS---------TSSHLPNLME---------- 490
PUT5_At1g19553      RFIPEETRPVSGVSSESQLDEEHGDESAASLLP 479
PUT4_At3g13620      EFN--------EVIDDLDNNVNGEHPKVDDHNS 478
```

[α] The sequence is aligned by ClusterW software(http://www.ebi.ac.uk/Tools/msa/clustalw2/, Larkin et al., 2007).

Table 4. 2 Molecular formula of methyl viologen and its analog polyamines

Methyl viologen	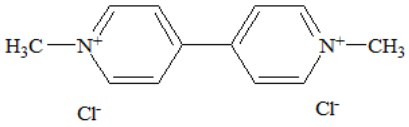
Putrescine	$[H_3N\text{-}CH_2\text{-}CH_2\text{-}CH_2\text{-}CH_2\text{-}NH_3]^{2+}$
Spermidine	$[H_3N\text{-}(CH_2)_4\text{-}NH_2\text{-}CH_2\text{-}CH_2\text{-}CH_2\text{-}NH_3]^{3+}$
Spermine	$[H_3N\text{-}(CH_2)_4\text{-}NH_2\text{-}CH_2\text{-}CH_2\text{-}CH_2\text{-}NH_2\text{-}(CH_2)_4\text{-}NH_3]^{4+}$

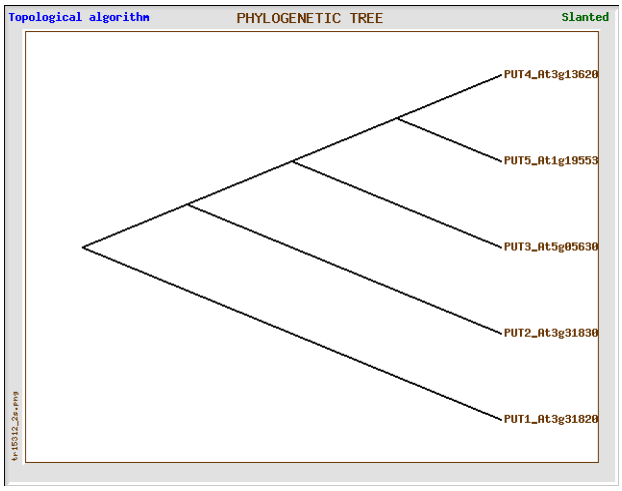

(A)

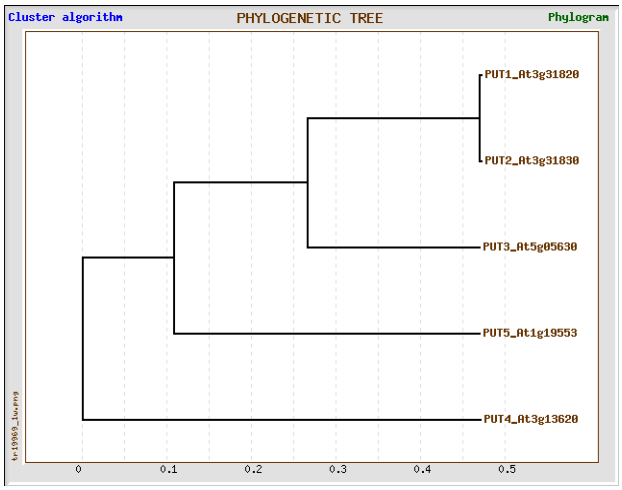

(B)

Figure 4. 1 Phylogenetic tree prediction of polyamine uptake transporter homologs in *Arabidopsis*. **(A)** Prediction in usage of topological algorithm. **(B)** Prediction in usage of cluster algorithm. The analysis was done by using genebee software (http://www.genebee.msu.su/services/phtree_reduced.html).

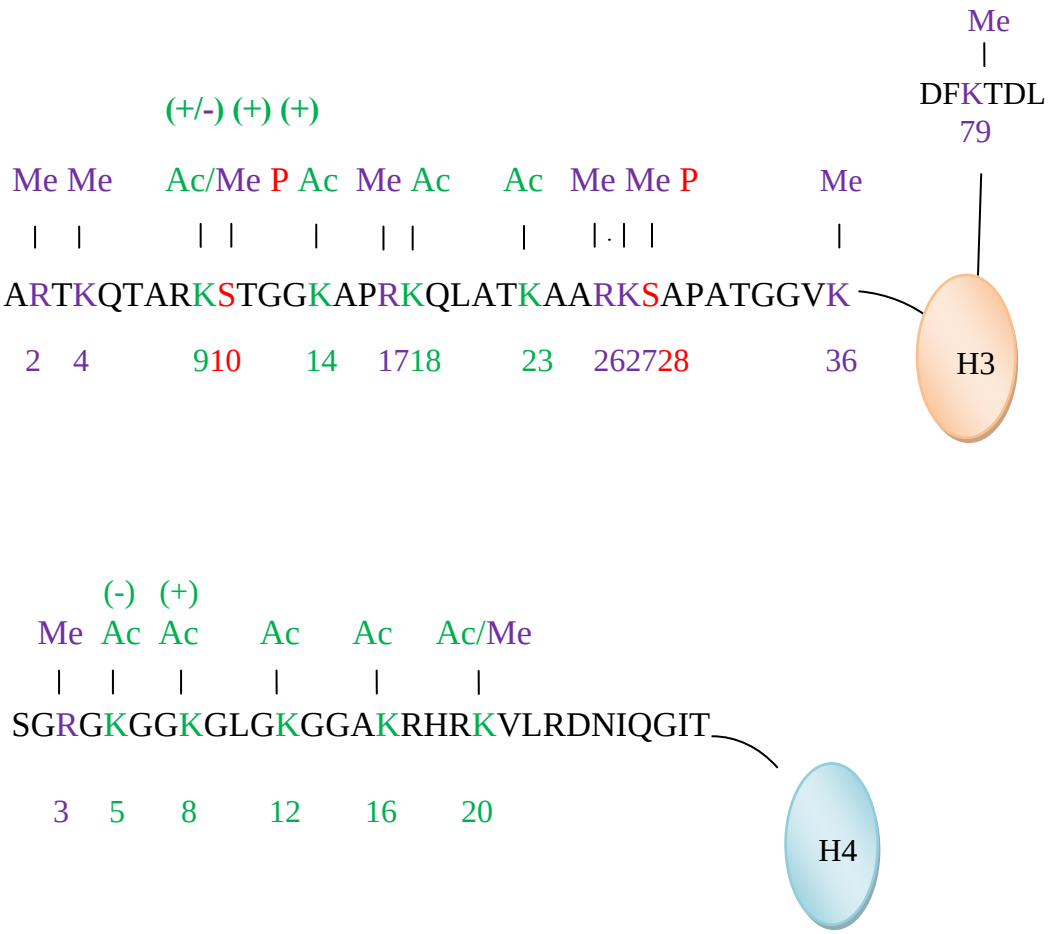

Figure 4. 2 Illustrations of post-modifications of amino acid residue on Histone 3 and Histone 4 in *Arabidopsis*. Ac: acetylation; Me: methylation; P: phosphorylation.

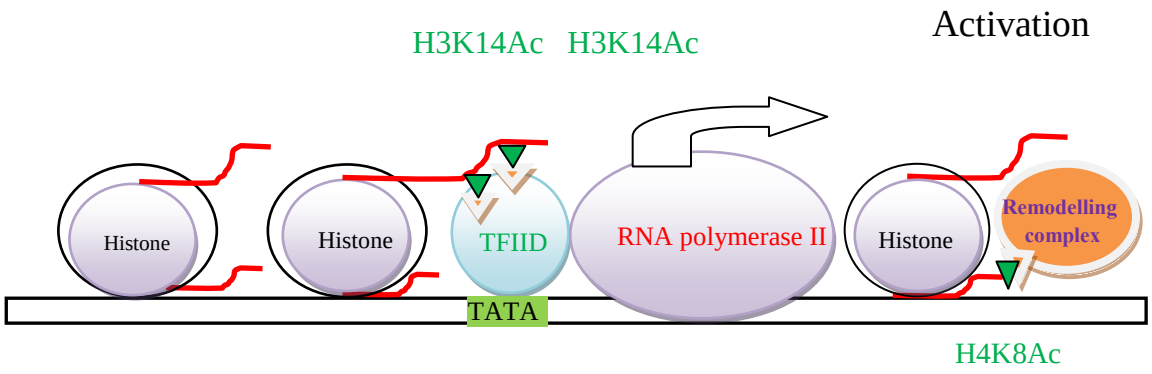

(A)

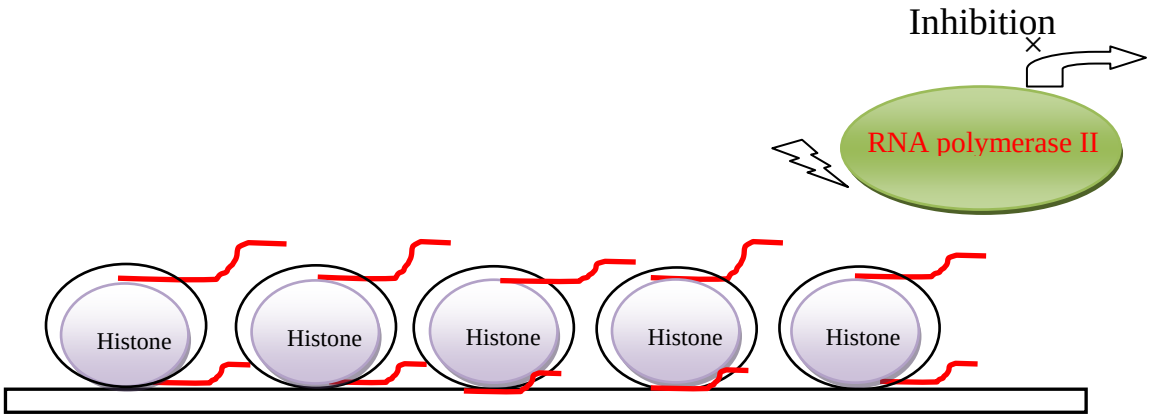

(B)

Figure 4. 3 Model of histoneacetylation affecting gene transcription. **(A)** Polyamines present enhance acetylation and transcription of genes. **(B)** Reduced polyamines lead to reduced histone acetylation and transcription of genes.

REFERENCES

Agalioti, T., Chen, G., and Thanos, D. (2002). Deciphering the transcriptional histone acetylation code for a human gene. Cell. **111**, 381-392.

Berger, S. L. (2002). Histone modifications in transcriptional regulation. Curr. Opin. Genet. Dev. **12**,142-148.

Deng, H., Bloomfield, V. A., Benevides, J. M., Thomas Jr, J. G. (2000). Structural basis of polyamine–DNA recognition: spermidine and spermine interactions with genomic B-DNAs of different GC content probed by Raman spectroscopy Nucleic Acids Res. **28**, 3379-3385.

Feder, M. E., and Hofmann, G. E. (1999). Heat-shock proteins, molecular chaperones, and the stress response: evolutionary and ecological physiology. Annu. Rev. Physiol. **61**, 243-282.

Feuerstein, B. G., Pattabiraman, N., Marton, L. J. (1989). Molecular dynamics of spermine-DNA interactions: sequence specificity and DNA bending for a simple ligand. Nucleic Acids Res. **17**, 6883-6892.

Fujita, M., Fujita, Y., Iuchi, S., Yamada, K., Kobayashi, Y., Urano, K., Kobayashi, M., Yamaguchi-Shinozaki, K., and Shinozaki, K. (2012). Natural variation in a polyamine transporter determines paraquat tolerance in Arabidopsis. Proc. Natl. Acad. Sci. U S A **109**, 6343-6347.

Georgopoulos, C., and Welch, W.J. (1993). Role of the major heat shock proteins as molecular chaperones. Annu. Rev. Cell Biol. **9**, 601-634.

Gernhard, S., von Koskull-Döring, P., Vierling, E., and Scharf, K. D. (2008). The plant sHSP superfamily: five new members in Arabidopsis thaliana with unexpected properties. Cell Stress and Chaperones. **13**, 183-197.

Goll, M. G., and Bestor, T. H. (2002). Histone modification and replacement in chromatin activation**.** Genes Dev. **16**, 1739-1742.

Hobbs, C. A. and Gilmour, S. K. (2000). High levels of intracellular polyamines promote histone acetyltransferase activity resulting in chromatin hyperacetylation. J. Cell. Biochem. **77**, 345-360.

Hirayama, T., Shinozaki, K. (2010). Research on plant abiotic stress responses in the post-genome era: past, present and future. The Plant J., **61**, 1041-1052.

Igarashi, K., Kashiwagi, K. (2010). Modulation of cellular function by polyamines. Int. J. Biochem. Cell Biol. **42**, 39-51.

Iwashita, Y., Sakiyama, T., Musch, M.W., Ropeleski, M. J., Tsubouchi, H., and Chang, E. B. (2011). Polyamines mediate glutamine-dependent induction of the intestinal epithelial heat shock response. Am. J. Physiol.Gastrointesine. Liver Physiol. **301**, G181-G187.

Kashiwagi, K., Kuraishi, A., Tomitori, H., Igarashi, A., Nishimura, K., Shirahata, A., and Igarashi, K. (2000). Identification of the putrescine recognition site polyamine transport protein PotE. J. Biol. Chem. **275**, 36007-36012.

Kim, B. H., Schoeffl, F. (2002). Interaction between Arabidopsis heat shock transcription factor 1 and 70 kDa heat shock proteins. J. Exp. Bot.**53**, 371-375.

Kodama, Y., Nagaya, S., Shinmyo, A., Kato, K. (2007). Mapping and characterization of DNase I hypersensitive sites in Arabidopsis chromatin. Plant Cell Physiol.**48**, 459-470.

Kotak, S., Larkindale, J., Lee, U., Von Koskull-Döring, P., Vierling, E. and Scharf, K.D.(2007). Complexity of the heat stress response in plants. Curr. Opin. Plant Biol.**10**, 310-316.

Krogh, A., Larsson, B., von Heijne, G., Sonnhammer, E. L. (2001). Predicting transmembrane protein topology with a hidden Markov model: application to complete genomes. J. Mol. Biol. **305**, 567-580.

Larkindale, J. and Knight, M. R. (2002) Protection against heat stress-induced oxidative damage in Arabidopsis involves calcium, abscisic acid, ethylene, and salicylic acid. Plant Physiol.**128**, 682-695.

Larkindale, J., Hall, J. D., Knight, M. R., Vierling, E. (2005b) Heat stress phenotypes of Arabidopsis mutants implicate multiple signalling pathways in the acquisition of thermotolerance. Plant Physiol.**138**, 882-897.

Larkin, M. A., Blackshields, G., Chenna, R., McGettigan, P. A., McWilliam, H., Valentin, F. Wallace, I. M. Wilm, A. Lopez, R., Thompson, J. D., Gibson, T. J., Higgins, D. G. (2007). Clustal W and Clustal X version 2.0. Bioinformatics **23**, 2947-2948.

Leutwiler, L. S., Hough-Evans, B. R., Meyerovitz, E. M. (1984). The DNA of Arabidopsis thaliana. Mol. Gen .Genet.**194**, 15-23.

Li, M., Berendzen, K.W., Schöffl, F. (2010). Promoter specificity and interactions between early and late Arabidopsis heat shock factors. Plant. Mol. Biol.**73**, 559-567.

Liu, H. T., Li, G. L., Chang, H., Sun, D. Y., Zhou, R. G., and Li, B. (2007). Calmodulin-binding protein phosphatase PP7 is involved in thermotolerance in Arabidopsis. Plant, Cell & Environment. **30**, 156-164.

Liu, H. T., Sun, D. Y., and Zhou, R. G. (2005). Ca^{2+} and AtCaM3 are involved in the expression of heat shock protein gene in Arabidopsis. Plant, Cell & Environment. **28**, 1276-1284.

Maher, L. J. (1998). Mechanisms of DNA bending. Curr. Opin. Chem. Biol. **2**, 688-694.

Meijer, H. J., Ter Riet, B., Van Himbergen, J. A., Musgrave, A. and Munnik, T. (2002). KCl activates phospholipase D at two different concentration ranges: distinguishing between hyperosmotic stress and membrane depolarization. Plant J.**31**,51-59.

Mishkind, M., Vermeer, J. E. M., Darwish, E., Munnik, T. (2009). Heat stress activates phospholipase D and triggers PIP2 accumulation at the plasma membrane and nucleus. The Plant J. **60**, 10-21.

Morgan, D. M. (1997). Measurement of polyamine transport: adherent cells. Polyamine protocols **79**, 139-147.

Morgan, D. M. (1999). Polyamines. An overview. Mol. Biotechnol. **11**, 229-250.

Nishizawa, A., Yabuta,Y., Yoshida, E., T. Maruta, Yoshimura, K., and Shigeoka, S. (2006). Arabidopsis heat shock transcription factor A2 as a key regulator in response to several types of environmental stress. The Plant J. **48**, 535-547.

Nover, L., Bharti, K., Döring, P., Mishra, S. K., Ganguli, A., Scharf, K. D. (2001) Arabidopsis and the heat stress transcription factor world: how many heat stress transcription factors do we need? Cell Stress and Chaperones. **6**, 177-189.

Pruitt , R. E, Meyerovitz, E. M. (1986). Characterization of the genome of Arabidopsis thaliana. J. Mol. Biol. **187**,169-183

Schwarzenbacher, R., Godzik, A., Jaroszewski, L. (2008). The JCSG MR pipeline: optimized alignments, multiple models and parallel searches. Acta Crystallogr D Biol Crystallogr. **64**, 133-140.

Strenkert, D., Schmollinger, S., Sommer, F., Schulz-Raffelt, M., and Schroda, M. (2011). Transcription factor-dependent chromatin remodeling at heat shock and copper-responsive promoters in Chlamydomonas reinhardtii. Genes Dev. **23**, 2285-2301.

Sun, Y., and MacRae, T. (2005). Small heat shock proteins: molecular structure and chaperone function. Cell Mol. Life Sci. **62**, 2460-2476.

Swindell, W., Huebner, M., and Weber, A. (2007). Transcriptional profiling of Arabidopsis heat shock proteins and transcription factors reveals extensive overlap between heat and non-heat stress response pathways. BMC Genomics **8**, 125.

Spyropoulos, I. C., Liakopoulos, T. D., Bagos, Pantelis. G and Hamodrakas, Stavros. J. (2004).TMRPres2D: high quality visual representation of transmembrane protein models.Bioinformatics. **20**, 3258-3260.

van Montfort, R. L., Basha, E., Friedrich, K. L., Slingsby, C., Vierling, E. (2001). Crystal structure and assembly of an eukaryotic small heat shock protein. Nat. Struct. Biol. **8**, 1025-1030.

Zhu, J. K. (2002). Salt and drought stress signal transduction in plants. Annu. Rev. Plant Biol. **53**, 247-273.

APPENDIX A

THE INTERACTING COMPONENTS LISTED IN THE NETWORKS OF FIGURE 1. 5

(B) At3g13445: TBP1 (TATA binding protein 1); CDC2: cyclin-dependent protein kinase; CRK2: calcium-dependent protein kinase, putative / CDPK; TBP2: TATA binding protein 2; HPPBF-1: telomeric DNA binding protein 1; PP7: serine/threonine phosphatase 7; HSC70-1: heat shock cognate protein 70-1.

(C) At4g15802: unknown protein; HSF1: heat shock transcription factor A-1a; ATHSFA2: heat shock transcription factor HsfA2.

(D) At4g15802: unknown protein; SUMO1: small ubiquitin-like modifier 1; ROF1: rotamase FKBP1; HSP83: ATHSP90.1, heat shock protein 90.1.